

Cold and Mortality in a Cross-Sectional and Lifecycle Perspective: Evidence from Competing Models *

Christian M. Dahl
University of Southern Denmark[†]

Martin Karlsson
University of Duisburg-Essen[‡]

Emil N. Sørensen
University of Southern Denmark[§]

Nicolas R. Ziebarth
Cornell University[¶]

February 17, 2019

Abstract

This paper models the relationship between cold and mortality using two competing modeling techniques and two unique datasets from Sweden. The first dataset is the Swedish mortality statistic at the county-month level by cause of death. Linear fixed effects models simulate the dominant modeling approach in the economics literature and serve as a benchmark. The second dataset comprises entire life spells of 30,150 Swedes who were born between 1930 and 1935. Along with daily temperatures over 84 years from 1930 to 2013, we then model the impact of exposure to extreme temperatures on cause-specific mortality over humans' lifecycle through competing risk models. In contrast to linear models, these models consider that temperatures can affect health through more than just one disease channel. Thus, the models allow time-varying temperature indicators to have competing effects on death due to heart diseases, respiratory diseases, and cancer. Although competing risk models have rarely been applied to this context, we show that they are a complementary modeling approach to study extreme temperatures and human health. Both modeling approaches find that extreme cold significantly increases the risk of dying from heart attacks. We compare both approaches and discuss possible biological mechanisms.

Keywords: population health effects, extreme temperatures, cold wave, weather, hospital admissions, mortality, climate change

JEL classification: I12, I18, Q54, Q58

*This is an early draft and all results are preliminary.

[†]University of Southern Denmark, Department of Business and Economics, Campusvej 55, DK-5230 Odense M, Denmark e-mail: cmd@sam.sdu.dk

[‡]Chair of Health Economics, Schützenbahn 70, 45117 Essen, Germany e-mail: martin.karlsson@uni-due.de

[§]University of Southern Denmark, Department of Business and Economics, Campusvej 55, DK-5230 Odense M, Denmark e-mail: emns@sam.sdu.dk

[¶]Cornell University, Department of Policy Analysis and Management (PAM), 426 Kennedy Hall, Ithaca, NY 14850, DIW Berlin, and IZA Bonn e-mail: nrz2@cornell.edu

[‡]We thank Therese Nilsson for making data for this research available and Thomas Longdens for an excellent discussion of the paper. We also thank participants at the Essen Health Conference 2018, in

1 Introduction

In the past decade, heat and cold waves have hit different regions of the world in regular and increasing intervals. These temperature extremes illustrate the relevance and challenges of climate change for humans (cf. [Peterson et al., 2013](#)). Not surprisingly, research on the relationship between temperature extremes and human health is a flourishing and diverse field in economics, public health and epidemiology. [Deschenes \(2014\)](#) provides an excellent overview.

Using a variety of datasets and methods, the general consensus across fields is that both extreme heat and extreme cold increase mortality. In economics, the standard methodological approach uses reduced-form OLS models and individual-level data with rich sets of region and time fixed effects (cf. [Deschênes and Moretti, 2009](#); [Deschênes and Greenstone, 2011](#); [Barreca et al., 2016](#)). In public health and epidemiology, the standard methodological approach uses poisson models and aggregated time-series rates or counts (cf. [Curriero et al., 2002](#); [Son et al., 2016](#)). [Karlsson and Ziebarth \(2018\)](#) apply and compare the performance of both approaches. One limitation of both literature strands is the focus on contemporaneous dose-response relationships and the estimation of short-term effects.

However, following [Grossman \(1972\)](#)'s human capital model, the focus in the empirical economics literature has shifted to a lifecycle perspective—and to estimating the impact of environmental conditions on human health in the long-run (cf. [Almond and Currie, 2011](#); [Graff Zivin et al., 2018](#)). For accurate predictions about the impact of climate change, learning more about the lifecycle health effects of environmental conditions is crucial.

The main contribution of this paper is to estimate the impact of extreme temperatures on mortality using novel lifecycle data and survival rate modeling approaches. We also compare the results from this novel approach, leveraging longitudinal data, to the dominant approach in the literature that uses cross-sectional data on mortality rates at given points in time. For that purpose, we exploit unique manually digitized longitudinal data that contain entire life spells from birth to death over more than 80 years. Specifically, we use individual-level data that track 30,150 Swedes from birth (in 1930-1935) until December 31st 2013 or death. For each individual,

particular Olivier Deschenes, for very helpful comments and suggestions. We also thank Ada Wossink and Toke Aidt for very helpful comments on earlier drafts. The research reported in this paper is not the result of a for-pay consulting relationship. Our employers do not have a financial interest in the topic of the paper that might constitute a conflict of interest. All remaining errors are our own.

we observe sociodemographic background information, gender, cause-of-death as well as the place of residency measured at several points throughout their lives. We link these unique life-spell cohort data to weather data on a daily level over the same time period, from 1930 to 2013. Next, we consider human migration over the lifecycle and create localized temperature exposure measures tailored to the relocation history of each individual. To our knowledge, this is the first paper to model temperature exposure over entire lifecycles of thousands of humans to assess its impact on health.

Methodologically, we apply a variety of hazard-based models to evaluate the dose-response relationship between weather exposure and different causes of death. We model contemporaneous weather exposure as a time-varying covariate in both a single-risk and a competing-risk framework. Both types of models use cause-specific and subdistribution-specific hazards in the context of semi-parametric proportional hazard models. In addition, we allow for unobserved heterogeneity over geographic locations of birth. Our analysis incorporates the relocation of humans over their lifecycles and the implied changes in weather exposure over time. This approach allows us to precisely measure and estimate the relationship between lifecycle exposure to cold and mortality. It also allows us to determine if such a relationship is homogenous across different causes of death.

Before we propose competing risk models to study the link between exposure to extreme temperatures and cause-specific risks of dying over the lifecycle, we run standard models as a benchmark. Such standard models typically rely on administrative mortality statistics at the regional monthly or even annual level. Then researchers regress the death rate on sets of time and region-fixed effects, along with a series of temperature bins which represent the distribution of average monthly or annual temperatures. We use Swedish administrative mortality data on the county-month level to simulate that approach in a first step.

In the next step, we demonstrate that competing risk models are a suitable modeling approach to study time-varying dose-response relationships, especially in a lifecycle perspective. However, the economics literature has rarely applied them to model the relationship between extreme temperatures and human health. (Notable exceptions are [van den Berg et al. \(2006\)](#), [van den Berg et al. \(2011\)](#), and [Yeung et al. \(2014\)](#) who apply hazard models to study the impact

of economic shocks during childhood on mortality later in life.¹) The modeling of competing risks and cumulative incidences is a void that this paper intends to fill. Hazard-based models allow the inclusion of individual-level characteristics, can deal with censoring, and make it possible to account for the competing nature of mortality risks. For example, dying early from pneumonia precludes the occurrence of late-life deaths due to heart attacks. Consequently, the impact of living conditions on pneumonia risks matters for the assessment of heart attack risks, and vice versa. Further, as we will show, it is straightforward to incorporate time-varying exposure to living conditions. We will investigate how such covariate paths relate to mortality due to extreme cold. We also apply extensions to model correlated lifetime events and unobserved heterogeneity.

Our findings show, first, that both modeling techniques, despite using differently structured data and functional forms, yield qualitatively comparable results. Both approaches produce a significant relationship between mortality and periods of extreme cold, such as the 2019 cold wave in North America. Second, the aggregated county-month level models yield a significantly, 10% higher, mortality rate during cold waves, which defined as days with temperatures in the 1st percentile of the local historical temperature distribution. Third, the individual-level competing risk models find that the overall risk of dying is 1.5 times higher during periods of extreme cold. Fourth, extreme cold is related to mortality due to several causes. In particular, both datasets and approaches reveal a clear increase in the mortality risk due to acute myocardial infarction (AMI, “heart attacks”). The individual-level data find similar effects for various cancer endpoints (gastrointestinal, genital, lung and other cancers). We also find that the effect is driven by late-life outcomes rather than child mortality. Fifth, the competing risk framework allows us to show the robustness to alternate model specification, including when accounting for unobserved heterogeneity at the parish-level and considering human migration over their lifetime. Finally, consistent with the “harvesting hypothesis” (Deschênes and Moretti, 2009), the cold effects for cancer dissipate after 10 days, while they persist for heart attacks, implying a persistent mortality response.

The current version of this paper does not investigate the specific but important issue of cold exposure to adverse *in utero* or early childhood conditions (see e.g. van den Berg et al.,

¹Outside of economics, Dockery et al. (1993); Lepeule et al. (2006), van den Berg et al. (2009), van den Berg et al. (2011), and Bruckner et al. (2014) represent additional noteworthy examples of hazard-model applications related to this paper.

2011, 2006; Currie et al., 2014; Zivin and Shrader, 2016). However, our models do account for unobserved differences in mortality due to variation in the local region of birth. Hence they implicitly consider differences in *in utero* weather conditions (Wilde et al., 2017).

Section 2 discusses the data used for the analysis. We also elaborate on our procedures to account for human migration and describe how we operationalize the weather data. Section 3 outlines how we model competing risks. Next, Section 4 presents and discusses the main results. The final section concludes.

2 Data

The empirical analysis makes use of two main datasets. We produce these two main datasets by combining each (a) the Swedish mortality statistic and (b) 84 years of individual-level lifecycle data with (c) temperature data. The mortality data cover the time period from 1968 to 2012 and records all deaths, along with its cause, at the county-month level, see Heckley et al. (2018) for a detailed discussion of the dataset. The lifecycle data track Swedes born in the 1930s over their lifetime and records cause-of-death and socio-demographic background information, see Bhalotra et al. (2017) for a detailed discussion. The weather data allow us to link the mortality statistic to contemporaneous temperatures and also to reconstruct temperature exposure histories for each of the thousands of individual lifecycle spells.

After briefly describing the aggregated mortality and individual-level lifecycle data, we explain how we converted the raw temperature data into lifecycle exposure histories. We also explain how we account for individuals' migration pattern over their lifecycle to measure lifecycle exposure to ambient weather conditions.

2.1 Mortality Rates at the County-Month Level from 1968 to 2012

The administrative mortality data are from the Swedish Interdisciplinary Panel (SIP).² It includes the universe of deaths in Sweden between 1968 and 2012, by county and month-of-the-year. Importantly, the data include the cause of death. Depending on year of death, the underlying cause of death is recorded according to the 7th, 8th, 9th and 10th versions of the In-

²It is based on Statistics Sweden's Multiple Generation dataset to which all other datasets are then linked using personal identifiers. It is administered at the Centre for Economic Demography, Lund University, Sweden and approved by the *Lund University Regional Ethics Committee, DNR 2013/288*.

ternational Classification of Diseases (ICD). We extract the most common causes of death and define and categorize them consistently over time.³ (Table A3 in the Appendix shows the exact categorization by ICD codes.)

- **Heart-attack:** acute myocardial infarction.
- **Other heart:** other cardiovascular diseases (*excl. AMI and cardiac arrests*).
- **Respiratory:** respiratory diseases.
- **Lung Cancer:** lung cancers.
- **GGI Cancer:** genital and gastrointestinal (GGI) cancers.
- **Other Cancer:** other neoplasm (*excluding lung and GGI cancers*).

Next, we sum over all deaths in a given county and month-of-the-year, and normalize the absolute number of deaths by the contemporaneous population at the time. In total, this yields 12,384 county-month mortality rates. Table 1 shows the summary statistic. As seen the all-cause mortality rate is 31.37 per 100,000 population. Death due to heart diseases represent the biggest fraction of death (8.24 per 100,000) where death due to acute myocardial infarction (“heart attacks”) is the single most important subcategory with 1.71 deaths per month and 100,000 population. The table also shows the other cause-specific death rates due to respiratory diseases (0.57), lung cancer (0.59), GGI (0.69) and all other causes.

2.2 Lifecycle Data at the Individual-Level over 84 Years

Our second and main dataset consists of 30,150 individuals, who are representative of each cohort born between 1930 and 1935 in Sweden. The dataset has been assembled by manually digitizing historical records from Swedish administrative and school archives. It contains detailed background information and allows us to reconstruct lifetime spells based on birth and death dates.⁴ The lifetime spells run from birth between 1930 and 1935 to either (i) death or (ii) the end of the study period in December 31st, 2013. The oldest individuals in the sample (and consequently the longest durations) are approximately 84 years old.

³The categorization is also motivated by findings in the literature. For example, [van den Berg et al. \(2011\)](#) shows that unexpected adverse economic shocks increase cardiovascular deaths, but not deaths due to cancer. [Bruckner et al. \(2014\)](#) shows that an interaction of warm gestation and post-natal cold weather increases the risk of dying from ischemic heart disease, whereas no effect was found for strokes. Death due to respiratory diseases have also been linked to extreme temperatures (see eg. [Donaldson and Keatinge, 1997](#); [Deschenes, 2014](#)).

⁴Only for four individuals, the complete date-of-birth information is missing; hence the actual number of lifetime spells used is 30,146.

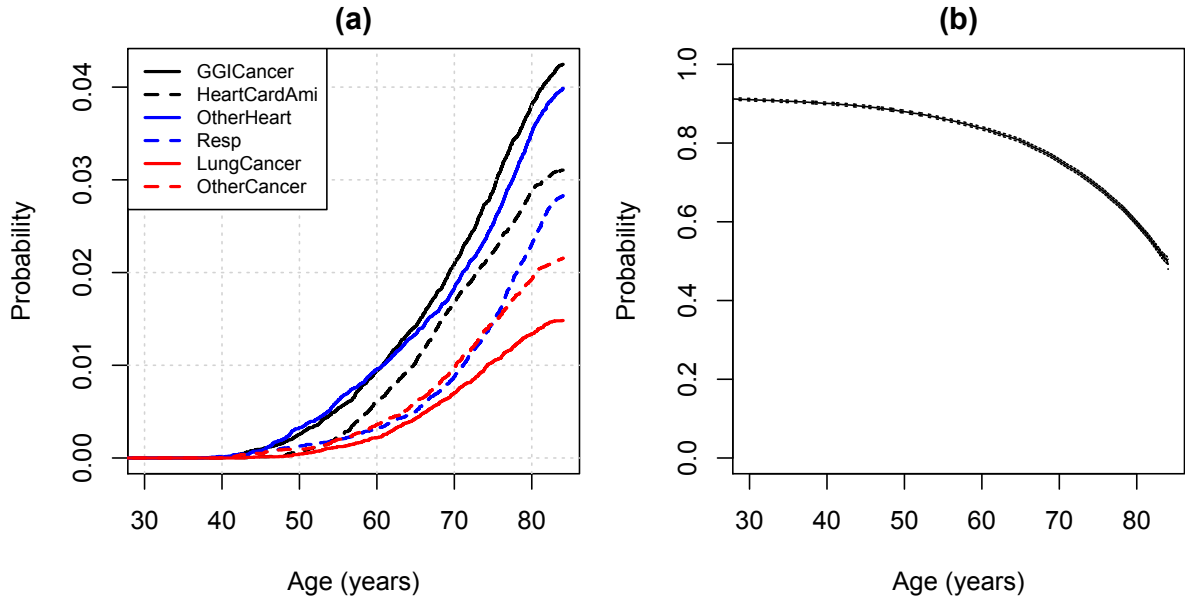
Because the lifecycle histories of the cohort have been manually researched in archives, the data are free of common issues in longitudinal data, e.g., sample attrition or survey non-response. However, for those individuals who had not died by December 31st, 2013, lifetime spells are right-censored. Section 3 we will elaborate on how we model censoring.

As with the SIP data above, when individuals died, we know the cause of death according to the International Classification of Diseases (ICD) and the two coding systems ICD-9 and ICD-10. We extract and categorize the same six causes of death as above. Note that even though we do not model all finer-grained causes of death explicitly, we consider the “residual” causes when we model cumulative incidence functions in Section 3.2.2.

Table 2 shows the summary statistic of the event types (causes) and their frequency. Interestingly but maybe not surprisingly, the distribution of cause-specific deaths differs between the aggregated and the cohort-level data. Differences in cross-section vs. longitudinal death probabilities already let us anticipate that the quantitative findings might differ in the Results section below. For example, in the cohort-level data, death due to GGI cancers represent the largest death risk over time with 10% of all observed deaths, whereas it solely accounts for about 5% of the total death rate in the cross-sectional perspective. Table 2 shows that death due to “other heart” diseases is the second largest death risk at around 9%, followed by heart attacks with 7% of all observed deaths. Note that over half of the cohort’s individuals were still alive on December 31st 2013;

The non-parametric estimates of the cumulative incidence functions in Figure 1 (left panel) provide information on the timing of the events for each cause of death in Table 2. These are estimated using the usual Aalen-Johansen estimators (Beyersmann et al., 2011). Notice that the incidences of all the remaining death causes are not plotted, instead we present the survival curve for staying in the initial state (alive) in the right panel of Figure 1. It is readily seen that death from the selected causes primarily occurs from age 45 and onward, which implies that our analysis focuses on the association between late-life mortality and exposure. Also, the timing of events appears similar across causes with the steepest changes in incidence around the age of 60-75. Respiratory diseases deviate somewhat with a steeper increase at high ages > 75.

Figure 1: Non-parametric cumulative incidence functions and survival in initial state



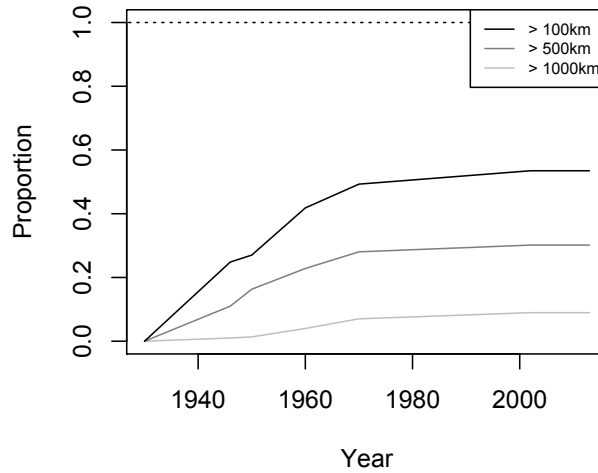
Source: Lifecycle data, own calculation, own illustration. Panel (a) presents non-parametric estimates of the cumulative incidence functions $F_k(t) = \mathbb{P}(T \leq t, \kappa = k)$ using the usual Aalen-Johansen estimators \hat{F}_k . Panel (b) shows the survival in the initial state (alive). Notice that the data in both plots have been truncated at age 30 as very few of the events occur prior to this age.

2.3 Relocation History and Imputation

This section explains how we model relocation of individuals over the lifecycle to assign temperature exposure more accurately. The contemporaneous place of residence determines contemporaneous temperature exposure. Relocation dates, on the other hand, indicate when individuals can experience abrupt changes in weather and ambient temperature when they move to locations with significantly different weather conditions. In Sweden, there are large discrepancies in weather between the Northern and Southern regions, so individuals could potentially move from a relatively warm county to a county with very cold temperatures.

The Swedish lifecycle data provide geocodes on living locations, taken at several predefined dates, namely at birth, 1946, 1950, 1960, 1970 and every year from 2000 to 2013. Because Sweden is subdivided into numerous ($N = 2,500$) small parishes, the residencies are recorded in geographic coordinates (latitude/longitude) and provide the distance to the nearest parish centroid.

Figure 2: Relocation over the lifecycle



Source: Lifecycle data, own calculation, own illustration. Figure shows the cohort share that has moved more than 100km, 500km or 1000km. Note that we only observe residences of individuals at birth and in 1946, 1950, 1960, 1970, 2002-2013. The exact relocation date is unknown.

Figure 2 illustrates the prevalence of human relocation within Sweden over the lifecycle. Around 25% of the cohort moved more than 500 km in their lifetime. Generally, humans tend to move early in life; only a small fraction moves after 1970, that is after their mid-30s. To consider changes in individual temperature exposure due to migration, we construct local temperature exposure series for each of the 30,150 individuals (see Section 2.4).

To assign moving dates, there are essentially two options: (a) assume people stay in their last known location until a new location is observed at the beginning of the years 1945, 1950, 1960, 1970, 2000-2013, or (b) impute the moving dates based on the known locations in 1945, 1950, 1960, 1970, 2000-2013. For now, we have voted for the imputation approach. We carry out the imputation using a random variable which is uniform on the discrete set of dates over the known dates. For example, if we know that an individual lives at location A in 1945 and in location B in 1950, then we impute the moving date by randomly drawing a date from the uniform set $\{01/01/1945, 02/01/1945, \dots, 31/12/1950\}$. We perform this imputation over every pair of years for which we observe a change in location. The imputed dates then constitute the moving history.

2.4 Weather Data

We use the weather data to assign individuals' contemporaneous and previously experienced temperature conditions.⁵ The raw data consists of temperature measurements from ambient weather monitors throughout Sweden. By merging historical and recent data, all of which are obtained from the Swedish Meteorological Service (SMHI), the measurements date back to the year 1800.⁶ Temperature is measured at a frequency of four hours and every measurement links to the latitude and longitude of the ambient weather monitor.

During our main study period from 1930-2013, new monitors appear and old ones shut down. This creates changes in geographic coverage and leads to missing observations. Figure 3 shows plots of active station grids for the years 1930, 1945, 1950 and 1970. As seen, the station grid is sparse around World War II and coverage is rather thin in the Northern regions during the first half of the 20th century. However, the grid becomes increasingly dense as we move towards the 1970s. (Note that our main events of interest occur after the age of 40 and thus after 1970 for most individuals.)

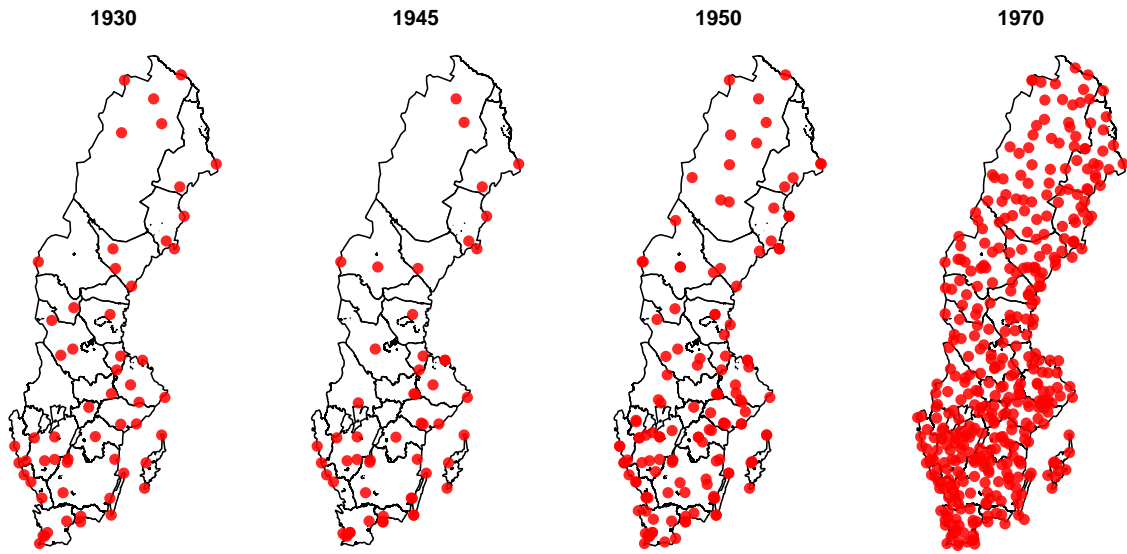
For the aggregated mortality data, we use the county where individuals died to assign average temperature conditions of that given month of the year in that given county of Sweden. In particular, we assign the number of extreme temperature days that represent cold waves (see Section 3 for the definition).

For the lifecycle data, we construct a temperature series that considers migration over the lifecycle for each individual as follows: We first convert the daily 4-hour temperature measurements into a 24-hour average, which yields a daily temperature series for each station. Next, we construct a local temperature series for each centroid of each parish. This gives us a new grid of measures that are compatible with the format of our relocation histories. Obviously, we need a complete parish temperature series from January 1st 1930 to December 31st 2013. For this purpose, we apply nearest-neighbor matching to assign each centroid measures from the next active monitors. Specifically, for each parish centroid, we determine the 5 nearest *active*

⁵In fact, the data not just contain temperature, but also precipitation, wind speed, cloud coverage, and maximum as well as minimum temperatures. For now, we are solely interested in ambient temperature, see e.g., Section 3.2 of Deschenes (2014).

⁶The recent data are accessible online, see <http://www.smhi.se> for details.

Figure 3: Distribution of ambient weather monitors over time



Note: Figure shows the weather station grid in 1930, 1945, 1950 and 1970. Noteworthy is the sparse grid around World War II and the large expansion in the following years, e.g., 1950 and 1970.

monitors in haversine distance. Then we average over the daily temperatures for these five stations.⁷

Obviously, with a sparser station grid, the temperature assignments are less precise. However, note that we never observe the exact residencies of individuals, only the centroid of their parish. In addition, following the literature, we approximate exposure to ambient temperatures by measured ambient temperatures. These caveats in the approximation of temperature assignment, for example, coarse resolution in geographical position will likely outweigh potential improvement in precision when applying alternative extrapolation methods such as kriging.

After having created comprehensive temperature times series for each parish from 1930 to 2013, we use the imputed moving history (see Section 2.3) to generate individual temperature exposure histories over the lifecycles of 30,150 individuals. As will be discussed in Section 3, we also construct “after-death” temperature series for all individuals who died before December

⁷We determined the optimal nearest-neighbor count through a standard 10-fold cross-validation scheme. Specifically, we omitted some monitors and used the remaining monitors to predict the temperatures of the omitted stations. We obtain the lowest cross-validation error with the 5 nearest neighbors.

31st 2013. We do so by assuming that individuals would have stayed in their last known living location and that they experienced the weather indefinitely after death.

3 Empirical strategy

We begin this section by briefly describing the conventional models in the economics literature to model the relationship between temperatures and mortality. Next, we describe in detail how competing risk models leverage the unique life cycle data to model the lifecycle impact of temperature exposure on different deadly diseases.

3.1 Linear Models for Mortality Rate Data

The dominating model in the economics literature uses aggregated mortality rates at the region-month or region-year level (cf. [Deschênes and Moretti, 2009](#); [Deschênes and Greenstone, 2011](#); [Barreca et al., 2016](#)). Then these rates are regressed on temperature bins and rich sets of spatial and temporal fixed effects:

$$Y_{cm} = \alpha + \sum_{h \in \{<10, 10-20, \dots, >80\}} \beta_h MeanTemp_{cm}^h + \sum_{j=2}^{25} v_j county_j + \sum_{m=Feb1968}^{Dec2012} \sigma_m month_m \quad (1)$$

$$+ \theta X_{ct} + \sum_{i=1}^{12} \sum_{h \in \{<10, \dots, >80\}} \gamma_{hi} MeanTemp_{c,m-i}^h + \epsilon_{cm}$$

where Y_{cm} denotes the mortality rate per 100,000 population in county c and month m . $MeanTemp_{cm}^h$ are temperature bins that equal 1 if the average monthly temperature in the county falls into a bin of 10 ° F and equal zero otherwise. The temperature coefficients then semiparametrically describe the temperature-health relationship, net of seasonal influences. We call this the “temperature bin model”. By contrast, the “threshold model” would replace $MeanTemp_{cm}^h$ with a main regressor indicating the share of *Cold Days* in month m of county c . Below we discuss how we define the number of cold waves as well as cold waves.

To account for the serial correlation in temperature, sometimes researchers add lags of $MeanTemp_{cm}^h$ to the model. While these lags are optional, the models routinely include county fixed effects, $\sum_{j=2}^{25} v_j county_j$ and year-month fixed effects, $\sum_{m=Feb1968}^{Dec2013} \sigma_m month_m$, to adjust for

trends and permanent differences in health across counties. Typically, the models also include time-varying county-level controls, X_{ct} and cluster standard errors at the county level. In most cases, Equation 1 would be weighted by the county population in a given year to attach more weight to more populous counties.

3.2 Competing Risk Models for Lifecycle Data

As pointed out by Deschenes (2014), although equation 1 is the dominant model in the economics literature, there exist alternative approaches to model the relationship between temperature exposure and mortality. Competing risk models also allow for time-varying covariates. In our main models, as discussed below, we will use the threshold model and include time-varying cold day threshold indicators (cf. Bruckner et al., 2014; Lepeule et al., 2006).

In contrast to the linear mortality rate model in equation 1, competing risk (or hazard or duration) models focus on the *duration* during which individuals live—and then model the hazard that life ends due to competing causes of death. The models assess how exogenous time variation in ambient temperatures affect the conditional distribution of such event-specific durations, while accounting for censoring (see Section 2.2) and individual characteristics. In other words, a competing risks model describes the time spend in an initial state (“being alive”) until transitioning into an absorbing endpoint of a particular type (“death due to a specific disease”).

The workhorse model of survival analysis is the proportional hazards model, usually in the form of a Cox regression (Cox, 1972). In our case, we will apply a “subdistribution model” as initially proposed by Fine and Gray (1999), which models the effects on the cumulative incidence function directly.⁸ The cumulative incidence incorporates changes in the likelihood of failure (“death”) not only as direct effects of a covariate, but also through the effect of this covariate on the risk for other endpoints; in other words, dying from alternative diseases. For example, cold might affect the risk of dying not only through an increased risk of heart attacks, but also through a reduced risk of strokes. There are several ways to model the cumulative incidence function—the most popular approaches are subdistribution models as pioneered by Fine

⁸Disentangling the effects of a specific covariate (e.g. temperature exposure) in a cause-specific hazards analysis can be challenging. Usually auxiliary techniques are necessary to obtain the full (or a *fuller*) picture, see Chp. 5 of Beyersmann et al. (2011).

and Gray (1999). In general, we formulate a standard competing risks model which, however, slightly differs from the “latent failure time framework” (Lancaster, 1992).

We now introduce the statistical setup. Assume that for each individual $i = 1, 2, \dots, n$ there exists a duration \tilde{T} , which is the time elapsed from birth until death from a specific cause in $\mathcal{K} = \{0, 1, 2, \dots, K\}$, with the cause-of-failure κ taking values in \mathcal{K} . In our data, we observe a (possibly right-censored) duration $T \equiv \min(C, \tilde{T})$, where C can be fixed or random.⁹ For right-censored observations, $C < \tilde{T}$, we set $\kappa = 0$. The duration T is measured on the age time scale such that all individuals enter at birth with $t = 0$. (This results in a staggered entry design, as those born between 1930 and 1935 are re-aligned at 0 when entering the study.)

Importantly, the covariate path for the individual’s lifecycle weather exposure is $Z_T = \{Z(t) : 0 \leq t \leq T\}$ where $Z(t)$ denotes the exposure at t and is a temperature indicator process with threshold values for *Cold Days*. In other words, if $\tilde{\tau}$ is a temperature cutoff and $\tau(t)$ the temperature (local to the individual) at time t , then $Z(t) = I(\tau(t) < \tilde{\tau})$ with I being an indicator function. In addition, we observe a time-constant covariate vector $\mathbf{X} \in \mathbb{R}^p$. Thus, for each individual, we observed the data tuple $(T, \kappa, \mathbf{X}, Z_T)_i$.

3.2.1 Cause-Specific Analysis

The cause-specific analysis specifies a model for each cause. In other words, it specifies models for the K hazards

$$a_k(t | \mathcal{D}) = \lim_{\delta \rightarrow 0} \frac{1}{\delta} \mathbb{P}(t < T \leq t + \delta, \kappa = k | T > t, \mathcal{D}) \quad (2)$$

where \mathcal{D} denotes conditioning random variables. Failures from all causes other than the modeled hazard are treated as right-censored. (When we assume no common effects across the k risks, we can motivate this approach through factorization of the likelihood function.¹⁰) We

⁹One the crucial assumption is that censoring is non-informative, see the elaborate treatment in (Andersen et al. (1993)) In our particular case, we have administrative censoring (“progressive type-I scheme”), so $C = c$ is known for all individuals.

¹⁰Consider the likelihood for all K cause-specific hazards, where we trivially obtain

$$L(\boldsymbol{\theta}; \mathbf{T}) = \prod_{k=1}^K \prod_{i=1}^n \exp(A_k(T_i; \boldsymbol{\theta})) a_k(T_i; \boldsymbol{\theta})^{I(\kappa=k)} = \prod_{k=1}^K L_k(\boldsymbol{\theta}; \mathbf{T})$$

such that $L_k(\boldsymbol{\theta}; \mathbf{T}) = \prod_{i=1}^n \exp(A_k(T_i; \boldsymbol{\theta})) a_k(T_i; \boldsymbol{\theta})^{I(\kappa=k)}$ is the likelihood for a proportional hazards model where everything but the type- k events are treated as right-censored. A_k is the cumulative hazard and a_k the hazard for k .

also impose the usual proportional hazards assumption. More formally, we consider the cause-specific hazard a_k for each risk $k \in \mathcal{K}$ to follow the proportional hazards form

$$a_k(t | \mathbf{X}, Z(t)) = a_{0k}(t) \exp(\beta_k \mathbf{X} + \zeta_k Z(t))$$

where a_{0k} is some unspecified baseline function. For a given risk k , we treat all observations with $\kappa \neq k$ as censored and estimate (β_k, ζ_k) with the Cox partial likelihood for time-varying “bounded and predictable” covariates ([Andersen et al. \(1993\)](#) and Chapter 6 of [Martinussen and Scheike \(2006\)](#)):

$$L_k(\beta_k, \zeta_k) = \prod_{t \in \mathcal{T}} \prod_{i=1}^n \left[\frac{\exp(\beta_k \mathbf{X}_i + \zeta_k Z_i(t))}{\sum_{j \in \mathcal{R}(t)} \exp(\beta_k \mathbf{X}_j + \zeta_k Z_j(t))} \right]^{I(\kappa_i = k)} \quad (3)$$

where $\mathcal{T} = \{t_1, t_2, \dots, t_n\}$ is the set of all distinct event times. Here we use $\mathcal{R}(t)$ to denote the risk-set at time t which has the standard definition $\mathcal{R}(t) = \{i : t_i > t\}$ in that t_i is the observed failure time of individual i . (Note that only failures of the cause k contribute to the likelihood.)

For the interpretation of the cause-specific hazard, it is often useful to also consider the cumulative incidence function (CIF). Even if $\zeta_k = 0$ for a given k in the cause-specific analysis, we might have $\zeta_k \neq 0$ in the subdistribution hazard for the same risk, as we will discuss in [Section 3.2.2](#) below. The reason is that a covariate may not have a direct effect on event A , but decrease the risk of a competing event B . In that case, we obtain an insignificant effect of the covariate on the cause-specific hazard for A but a significant effect on the associated cumulative incidence function. The important take-away is to always supplement the cause-specific analysis with a subdistribution model (see [Chp. 5 of Beyersmann et al., 2011](#)).

3.2.2 Subdistribution Analysis

As before, let $k \in \mathcal{K}$ be the risk of interest, that is, the cause of death. We will now analyze the cumulative incidence function

$$F_k(t | \mathbf{X}, Z_t) = \mathbb{P}(T \leq t, \kappa = k | \mathbf{X}, Z_t)$$

associated with k . The cumulative incidence is has a direct and intuitive probabilistic interpretation in a competing risks setting: “Conditional on the covariates, what is the probability of having experienced a type k event by time t ?” ¹¹

[Fine and Gray \(1999\)](#) consider direct transformation models for the cumulative incidence F_k . In particular, they assume that for some increasing function g , we have $g(F_k(t | \mathbf{X})) = h_{0k}(t) + \beta_k \mathbf{X}$ with β_k being the parameters of interest and h_{0k} an unspecified baseline function. On the transformed scale we get a vertical shift interpretation, e.g. for two individuals with covariate vectors $\mathbf{X}_1 = \mathbf{x}_1$ and $\mathbf{X}_2 = \mathbf{x}_2$ we obtain $g(F_k(t | \mathbf{x}_1)) - g(F_k(t | \mathbf{x}_2)) = (\mathbf{x}_1 - \mathbf{x}_2)' \beta_k$. [Fine and Gray \(1999\)](#) focus on the loglog link $g(u) = \log(-\log(1 - u))$ corresponding to the proportional hazards model and apply the definition of the subdistribution hazard ([Gray, 1988](#)) to model the effects on the cumulative incidence function directly, see also [Scheike and Zhang \(2008\)](#) for other choices of g .

The subdistribution hazard for risk k , denoted λ_k , is the hazard for the subdistribution waiting time, see the canonical reference [Fine and Gray \(1999\)](#). Thus, it is defined by

$$\lambda_k(t | \mathcal{D}) = \lim_{\delta \rightarrow 0} \frac{1}{\delta} \mathbb{P}(t < T \leq t + \delta, \kappa = k | T > t \cup (T < t, \kappa \neq k), \mathcal{D}) \quad (4)$$

where \mathcal{D} denotes any conditioning random variables. From (4) it is clear that this hazard is a somewhat artificial construct. Within the framework of general multi-state models the competing risks model arises as a special-case with one initial state and K absorbing states ([Andersen et al., 1993](#); [Beyersmann et al., 2011](#)). Here, the cause-specific hazards naturally correspond to the transition intensities into each absorbing state for individuals residing in the initial state (have not yet failed), cf. (2). However, the subdistribution hazard for k describes the instantaneous transition rate into endpoint k for individuals that (a) *have not yet failed* or (b) *have failed from a competing cause $j \neq k$* , i.e. the failure rate for people that have possibly already failed. A direct intuitive interpretation of this is difficult, which is pointed out by eg. [Andersen and Keiding \(2012\)](#) and, although less clearly, the original authors [Fine and Gray \(1999\)](#). Thus, the subdistribution hazard is primarily interesting as a statistical device to examine the effects of covariates on the cumulative incidence and does not provide us with the usual relative risk interpretations of eg. a single-risk proportional hazards model.

¹¹It is feasible to estimate the cumulative incidence based on the cause-specific hazards, but it would entail modeling all cause-specific hazards (a_1, \dots, a_K) explicitly ([Beyersmann et al., 2011](#)). It is also a cumbersome approach when interested in a direct interpretation of how specific covariates affect the cumulative incidence of a given cause.

Consider (a_1, \dots, a_K) to be the cause-specific hazards, the key relationship between the cause-specific hazards, the subdistribution hazard and cumulative incidence is given by:

$$F_k(t | \mathbf{X}, Z_t) = 1 - \exp \left(- \int_0^t \lambda_k(s | \mathbf{X}, Z(s)) \, ds \right) \quad (5)$$

$$= \int_0^t \exp \left(- \int_0^u \bar{a}(s | \mathbf{X}, Z(s)) \, ds \right) a_k(u | \mathbf{X}, Z(u)) \, du \quad (6)$$

where $\bar{a}(t | \mathbf{X}, Z(t)) = \sum_{j=1}^K a_j(t | \mathbf{X}, Z(t))$ is the all-cause hazard, see Chp. 5 of [Beyersmann et al. \(2011\)](#). We see that the effect of a given covariate on the CIF is weighted according to a factor that depends on the all-cause hazard. This means that the CIF incorporates information about the effect of a given covariate across all risk $k \in \mathcal{K}$ when determining the impact of said covariate on the incidence for risk k . It is also clear that there is a direct relationship between the subdistribution hazard and the cumulative incidence, and hence it is straightforward to interpret the direction and significance of covariate effects on the cumulative incidence function.

In our case, the subdistribution hazard takes the usual (and convenient) proportional hazards form such that our model becomes

$$\lambda_k(t | \mathbf{X}, Z(t)) = \lambda_{0k}(t) \exp(\beta_k \mathbf{X} + \zeta_k Z(t)) \quad (7)$$

where λ_{0k} is the subdistribution baseline hazard, $Z(t)$ is the (predictable) cold exposure indicator at time t and \mathbf{X} is a vector of time-independent covariates (e.g., gender, quarter-of-birth etc.). Clearly, by (7), the hazard at time t depends *only* on the present value of Z such that we model a contemporaneous association only, this is similar to [Bruckner et al. \(2014\)](#); [van den Berg et al. \(2006\)](#)). It is important to notice that the crucial assumption of the proportional hazards model is of course *proportionality*. This implies that while the regressors can be time-dependent (like Z) we still assume that the effects (β, ζ) are constant over the chosen time scale, i.e. age, so extreme weather affects children, middle aged and old people equally. There is some evidence suggesting that we can interpret the Fine-Gray estimates as time-averaged effects, see e.g., the suggestive simulation results of [Graw et al. \(2009\)](#). This means that the cold exposure effect should essentially be viewed as an average effect across all ages, both young and old. Later on,

we will investigate whether this assumption is reasonable (see Section 4.5) and discuss possible remedies and how it impacts our results.

In relation to this, we should also note that by construction the Fine-Gray model is not appropriate for analyzing all risks $k = 1, 2, \dots, K$ simultaneously¹². Obviously, it should hold that $\sum_k F_k(t|\cdot) \rightarrow 1$ for $t \rightarrow \infty$ but this is not guaranteed. Fortunately, our analysis only considers a subset of the available risks and hence is very suited for the application of the Fine-Gray method.

The parameters of interest (β_k, ζ_k) in (7) can be estimated by maximizing the usual Cox partial likelihood (Fine and Gray, 1999). However, we need to accommodate for the presence of right-censoring and accordingly the specific censoring mechanism. Individuals in our sample are only censored when living beyond December 31st, 2013 (see Section 2.2) and there is no (or only negligible) loss-to-followup. This means that for each individual i we are able to calculate the exact time c_i at which they are right-censored by considering the duration between birth and end-of-study. In the literature this is known as progressive type-I censoring (Andersen et al., 1993, p. 138) and data subjected to this censoring mechanism are also known as censoring-complete data in the parlour of Fine and Gray (1999). Also, there is no left truncation. This simplifies the estimation of the model considerably as the censoring times are known even in the case where a competing event is experienced. This means that there is no need to simulate the risk-set and no need for inverse probability-of-censoring weighting. Instead we can utilize the Cox partial likelihood (3) under an expanded risk-set as shown by Fine and Gray (1999). This allows the usual semi-parametric estimation approach of Cox (1972) where the baseline is left unspecified, and also leads to asymptotic results equivalent to those for the usual Cox partial-likelihood estimator making inference straightforward. At any time t we consider the expanded risk-set $\tilde{\mathcal{R}}_t = \{i : T_i > t \cup (T_i < t, \kappa \neq k)\}$ and rely on (3) with $\tilde{\mathcal{R}}(t)$ in place of $\mathcal{R}(t)$ as described by Fine and Gray (1999). This is straightforward to implement through the `coxph` function from the `survival` package (Therneau (2015)) in (R Core Team (2016)).

The combination of right-censoring (whether random or administrative) with time dependent covariates (such as weather exposure, $Z(t)$) presents some specific challenges in subdis-

¹²See e.g., the discussion in Section 5.3.4 of Beyersmann et al. (2011) where it is argued that the proportional hazards assumption cannot hold for all subdistribution hazards simultaneously and, per the standard results on violation of the proportional hazards assumption, we should consider the estimates as time-averaged

tribution models – both from a theoretical and practical perspective, see e.g., [Latouche et al. \(2005\)](#); [Cortese and Andersen \(2010\)](#); Chapter 5, [Beyersmann et al. \(2011\)](#). In particular, assume an individual dies from a competing risk at time t and is administratively censored at time c where $c > t$. For the interval $[0; t]$ we observe the path of the covariate process Z but what about the path for $(t; c]$? The individual is still at risk in the interval $(t; c]$ so we also need data on Z for this period. More specifically, we need to know the value of Z at all distinct event times occurring later than t but before c . However, in practice the individual is already dead from a competing cause so how can Z be observed? The answer to this question depends on the type of time-dependence exhibited by the covariate. The crucial assumption in this regard is that Z is external, see Section 6 of [Kalbfleisch and Prentice \(2011\)](#) (or *ancillary* in the parlour of [Cortese and Andersen, 2010](#)), so that we can observe weather exposure even in the case where the individual has died from a competing cause. In essence, the stochastic process describing weather exposure cannot depend on parameters that enter our model for the failure times, or similarly, the future path of Z must not be affected by failures at an earlier time as described in Sec. 6.3 of [Kalbfleisch and Prentice \(2011\)](#). We are still able to conduct inference in the case where this condition is violated but we will not be able to predict probabilities as the usual relationship between the hazard and the survival function (or CIFs) is invalid.

On a practical note, the individuals have to move quite far to alter their exposure significantly (recall from Section 2.4 that we perform a nearest-neighbor averaging procedure when calculating the temperatures which smoothes the temperature surface). Also, we gather from Figure 2 that when people reach a certain age (30-40 years) only few people relocate.

3.2.3 Unobserved Parish Heterogeneity

To account for unobserved heterogeneity at the parish level, i.e., correlation between survival times of individuals within a parish, we allow for proportional differences in the subdistribution hazard across parishes. Cold/warm parishes might in general be less (or more) healthy to live in, which would induce systematic differences in mortality between areas with correspondingly few/many cold waves.

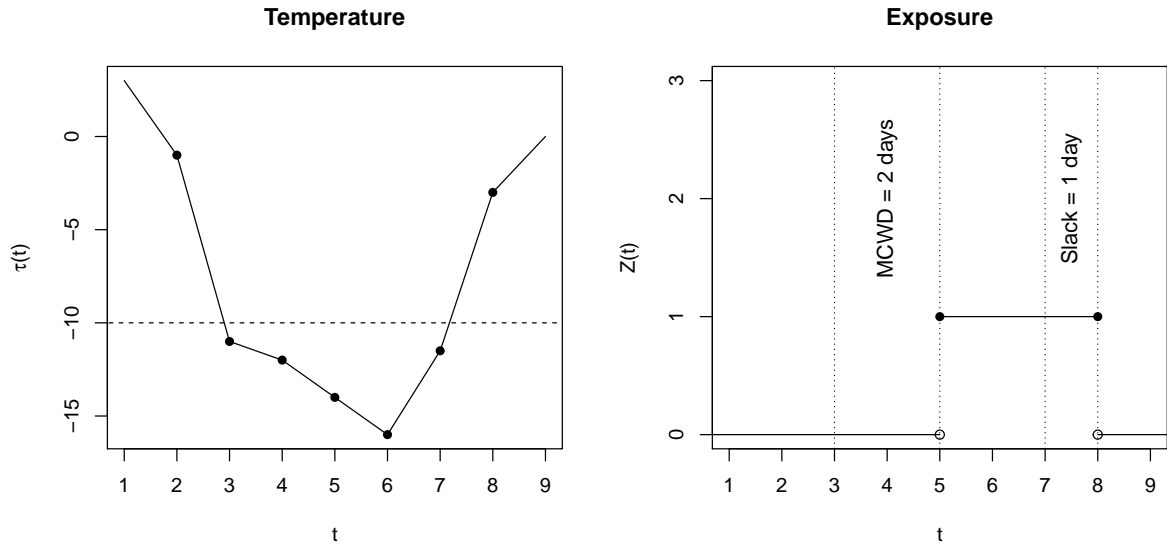
To an extent, this can be mitigated by allowing for parish heterogeneity using a shared frailty. Let the random variable V denote this frailty. Now the specification from (7) is conditional on V and our model becomes:

$$\tilde{\lambda}_k(t | \mathbf{X}, Z(t), V) = V \lambda_k(t | \mathbf{X}, Z(t)) \quad (8)$$

where the frailty distribution is chosen to be gamma such that $V \sim \text{Gamma}(\xi)$ with ξ being the frailty parameters. Each parish will carry a higher or lower hazard depending on the realized value of V and all individuals within a given parish will accordingly be subject to the same hazard scale factor. The frailty parameters ξ are estimated together with the covariate coefficients using a penalized partial-likelihood procedure, see e.g., [Ripatti and Palmgren \(2004\)](#). The `survival` package implements this procedure for R. Notice also that the specification in (8) assumes that parish heterogeneity is static and locked-in at birth. A dynamic perspective would more accurately reflect that people change parishes across their lifetime when relocating. An alternative modeling approach would be to incorporate time-changing strata, see [Zhou et al. \(2010\)](#) for the Fine-Gray setting. Modeling unobserved heterogeneity by parish membership at birth also serves to account for the effect of birth conditions on mortality, the existence of which has been well-documented in the literature, e.g., [van den Berg et al. \(2011, 2006\)](#). In particular, children within the same parish are likely to have experienced similar pre-birth and childhood conditions leading to systematic differences in survival across the birth parishes. Such within-parish correlation is also modeled by the frailty term V .

A related issue is modeling unobserved heterogeneity at the individual level which is prone to identification problems without multiple spells per subject (recurrent events) or paired designs (e.g., twins, as in [van den Berg et al., 2011](#)). Obtaining multiple durations for each individual is obviously infeasible when studying mortality, and hence it is disregarded in our setup. However, individual-level frailty (as will result if we have omitted variables) would generally create a selection effect where fragile individuals die early and leave a larger proportion of stronger survivors at older ages. This would downward bias the association between exposure and mortality at later-ages and thus we consider this less of a concern. Similar problems exist for competing endpoints where frailty is correlated across causes which can give rise to the false protectivity phenomenon. See Chapter 6 of [Aalen et al. \(2008\)](#).

Figure 4: Measuring cold day exposure



Note: The left panel displays the temperature time-series for a given individual in solid, where the dashed line marks the temperature threshold. Days with temperatures below the dashed line are defined as cold days. The right panel depicts the corresponding exposure indicator with the number of minimum consecutive wave days (MCWD) set to 2 and the slack set to 1 day. Note that the indicator only turns on after two days with cold weather have passed. It turns off with a delay of one day after the cold day. $Z(t)$ is graphed for a fictional temperature series.

3.3 Measuring Temperature Exposure

As described by [Deschenes \(2014\)](#), there are several approaches to measure temperature exposure. In Equation (7), it is a threshold indicator function which equals one for days with extreme cold. If there was an effect of cold on mortality, this would imply that the hazard at any t would be elevated by $\exp(\zeta_k)$ when the individual is exposed at time t .

Our threshold indicator approach is a slightly modified version of [Bruckner et al. \(2014\)](#). Recall that $Z(t)$ denotes temperature exposure at t and is defined as a binary temperature indicator for some threshold value. In other words, if $\tilde{\tau}$ is a temperature cut-off and $\tau(t)$ the actual temperature (local to the individual) on day t , then $Z(t) = I[\tau(t) < \tilde{\tau}]$, with $I[\cdot]$ being an indicator function. Thus, the parameter ζ for Z measures the association between extreme temperatures and the hazard rate.

Instead of choosing an absolute temperature threshold, we let $\tilde{\tau}$ be location-specific and equal to the 1st and 5th percentile of the all-time local temperature distribution, where local refers to Swedish parishes (cf. [Bruckner et al., 2014](#); [Deschenes, 2014](#)). Thus, for a given parish, temperatures below the 1st and 5th percentile are defined as cold days. In addition, we impose that an extreme cold event must at least have -15°C ([Medina-Ramón and Schwartz, 2007](#)).

Next, we introduce two extra conditions. First, we require a minimum number of consecutive days, where the temperature is below the threshold $\tilde{\tau}$ before we label the period as a *cold wave*. Second, we allow the indicator to stay on for a certain number of days after the last cold day. Specifically, let $m(t, j) = \sum_{b=0}^{j-1} \mathbb{I}(\tau(t-b) < \tilde{\tau})$ be the number of cold days in the past j days relative to time t . Then we define the Z cold wave indicator as:

$$Z(t) = \mathbb{I} \left[\sum_{b=0}^{\theta} \tilde{Z}(t-b) > 0 \right], \quad \tilde{Z}(t) = \mathbb{I}[m(t, \alpha) = \alpha] \quad (9)$$

where α denotes the number of minimum consecutive wave days (MCWD) and θ denotes the slack. Here, (α, θ) are “hyper” (or “tuning”) parameters that we select rather than estimate. [Figure 4](#) illustrates both the slack and MCWD parameters.

The MCWD requirement ensures that the temperature has persistently dropped below for several days. The slack day parameter θ allows for flexibility when linking extreme temperature to mortality; for example, when $Z(t) = 1$ and a death of type k occurs with a lag $t' > t$. In most cases, we will use a slack of 5-10 days. However, the main findings are fairly robust to the choice of θ .

[Figure 5](#) depicts the approximate share of cold days experienced by an individual relative to their observed lifetime. As seen, the slack indicator scales the distribution, but preserves the shape of the density. The peaks in all three plots are driven primarily by censored individuals, who have exactly the same lifetime duration from birth until the censoring date December 31st, 2013. [Figure 6](#) varies the minimum number of consecutive wave days and shows very similar densities.

Figure 5: Share of lifetime cold day under varying slack, θ .

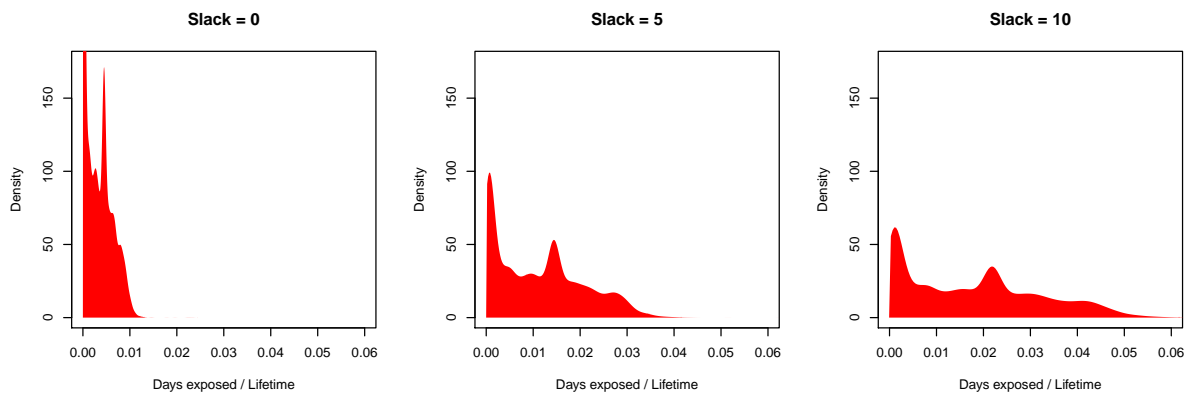
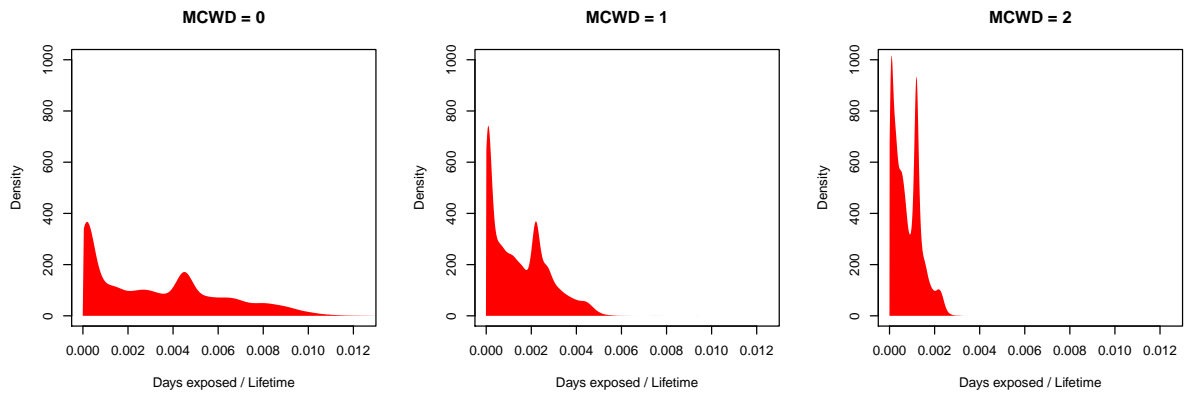


Figure 6: Share of lifetime cold days under varying minimum consecutive wave days (MCWD), α .



Note: Scale differs from Figure 5.

4 Results and Discussion

This section presents and discusses our main findings. First we briefly discuss the findings from our benchmark analysis, the standard approach in the economics literature to regress mortality rates on linear sets of region and time fixed effects. Then we comprehensively discuss the results for the competing risk analysis using lifecycle data and both cause-specific models as well as subdistribution models for the cumulative incidence. In all cases, we consider a relative percentile temperature threshold, as described in Section 3.3.

4.1 Linear Models for Mortality Rate Data

Table 3 shows the results when we estimate a linear model like in Equation (1). To recall, we use the universe of all Swedish death in a cross-sectional aggregated data design at the county-month level. These mortality rates are then linked to the number of cold days per month as described in Section 3.3 and shown in Figure 4. As in the competing risk analysis below we vary the slack day parameter θ between 0 and 10 days. Moreover, we show results for the 1st and 5th percentile of the all-time local temperature distribution and the location-specific threshold parameter $\tilde{\tau}$. Each panel and each column represents the findings from one separate model, where the column headers indicate the different causes of death.

In summary, Table 3 shows the following: First, the aggregated mortality data do not provide enough statistical power to estimate precise effects when we define cold days according to the 1st percentile of the local temperature distribution.

Second, when defining cold days according to the 5th percentile of the distribution, we consistently find a significant relationship between exposure to cold, all-cause mortality (column [1]), deaths due to heart attacks (column [2]) as well as death due to “other” heart diseases (column [3]).

Third, setting $\theta=0$, we find that a cold day raises the heart attack mortality rate by 7.1%, whereas setting $\theta=10$ yields an increase in the heart attack mortality rate by 3.9% (column [2]). For all-cause mortality, the effect sizes are 1% and 0.6%, respectively. These findings are entirely in line with Barreca et al. (2016); Deschênes and Moretti (2009); Deschênes and Greenstone (2011) and thus validate our benchmark analysis.

Fourth, although imprecisely estimated, we consistently find negatively signed relationships between cold and mortality due to respiratory diseases as well as cold and mortality due to GGI cancer. These suggestive relationships may be masked by important underlying cold-health channels. For example, it may only appear as though cold and respiratory health were negatively linked even though the relationship is actually positive. The reason could simply be that frail individuals with comorbidities who would have died of respiratory health issues die of heart attacks during cold waves. This illustrates the usefulness of competing risk analyses, which are powerful enough to unmask such relationships.

4.2 Competing Risk Models for Lifecycle Data

Our competing risk models follow Equation (7). However, the exact specification of the time-independent covariates \mathbf{X} varies as we consider two nested covariate configurations. Specification 1 solely incorporates temperature exposure and gender, but no frailty. In contrast, specification 2 contains temperature exposure, gender, twin birth (twin), quarter-of-birth (qBirth), birth year (bYear) and the mother's age-at-birth (mAgeB) as additional covariates. Specification 2 is estimated both with and without a frailty term V which is defined over the birth parishes.¹³

Recall that we model the cold impact on the following mutually exclusive (but non-exhaustive) causes of death: (1) heart attack (acute myocardial infarction), (2) other cardiovascular diseases (excluding heart attacks and cardiac arrest), (3) respiratory diseases, (4) lung cancer, (5) genital and gastro-intestinal cancer (GGI) and (6) other cancers. Even though we do not model all possible causes of death explicitly, we consider the remaining causes when we model the cumulative incidence functions. In what follows, we first briefly discuss the results for all-cause mortality and then proceed to the competing risks analysis.

4.3 All-Cause Mortality

As a simple point of departure, we begin by conducting a crude all-cause analysis where death from any cause is considered as an event. We estimate a Cox regression model that is functionally equivalent to the subdistribution model presented in (7) but for the all-cause hazard. The results for Specification 2 are presented in Table 4.

¹³We have also considered the mother's marital status and father's age-at-birth but found these covariates to be insignificant. Hence we excluded them from the final specifications.

We see a significant positive association between cold weather and mortality, which also holds if we condition on survival until the age of 40. This is in line with existing empirical evidence (Deschenes, 2014). The estimated effect of cold weather is approximately 1.5 which seems large in relative risk terms. However, we should keep in mind that we are looking across all causes and the effects on the cause-specific hazards (or CIFs) can therefore be both larger and smaller than this. Also, the estimated relative risk is confined to cold days, i.e. it does not make sense to think of an individual with $Z(t) = 1$ for all $0 \leq t \leq T$ as this would correspond to a person living in extreme cold their whole life. The estimate is an instantaneous and temporal effect on the hazard.

A competing risks analysis will help us determine whether Z has a homogenous association with mortality across causes. In particular, whether specific causes appear to be driving the results in Table 4.

4.4 Competing Risks with Relative Waves

This section considers the effects of cold exposure on the cumulative incidence functions. The temperature threshold is equal to the 1st percentile of the local temperature distribution with a maximum of $< -15^\circ\text{C}$. We add $\theta = 10$ days of slack to the indicator such that it stays on for 10 more days after the last cold day, see Section 3.3. The number of minimum consecutive wave days α is zero in all cases, meaning that we include cold spells as short as 1 day of length. The subdistribution hazard model in (7) is estimated for each of the selected causes using the survival package (Therneau, 2015) in R (R Core Team, 2016).

The parameters (β, ζ) in the model given by (7) are not easy to interpret quantitatively, rather they should be understood qualitatively. As is evident from Section 3.2.2 the coefficients signify the shift on a transformed scale. This means that they do not have the usual relative-risk interpretation from Cox regression, see Sec. 3 of Andersen and Keiding (2012) and Sec. 2 of Fine and Gray (1999). From a qualitative perspective we can consider the significance and sign of (β, ζ) as the subdistribution hazard λ_k is related to the CIF F_k according to (5), i.e. the sign is preserved. The main parameter of interest is of course the association between cold temperature and incidence as measured by ζ_k .

The results for Specification 1, which includes gender and exposure only, are presented in Table 5. The 0.95-confidence intervals and the significance marks are based on the non-

robust standard errors for the *transformed* coefficients, which relies on the proportional hazards assumption being satisfied. Notice that the event count for each cause is also given in the table, and that these differ slightly from those reported in Table 2 due to missing values. When comparing estimates across causes it is of course important to keep in mind that those with lower event counts will have larger standard errors and vice-versa.

Based on Table 5 there is strong evidence that cold exposure is significantly associated with increased incidence of death from heart-attacks, GGI and other cancers (excluding lung cancer). On the contrary, no effect is found for the other heart diseases, lung cancer and respiratory illnesses. This implies that there is heterogeneous effects of cold for different subgroups of cardio-vascular diseases, i.e. there is a clear association with heart-attack incidence but no relation with the remaining heart conditions. This is similar to the auxiliary result for continuous temperature exposure in Bruckner et al. (2014) where they find an effect for ischemic heart disease but nothing for strokes.

We now consider the extended Specification 2. The results are presented in Table 6. Comparing the exposure and gender coefficients with those of Specification 1, it is clear that these have changed only slightly with the addition of a frailty term and more controls (quarter-of-birth, birth year, mother's age-at-birth). If we look at the estimates for cold exposure under Specification 2, we gather from Table 6 that cold weather is still associated with a significant increase in mortality incidence for heart attacks, lung cancer, GGI cancer and other cancers, and that the (relatively) strongest relationship is seen for heart attacks. No association is found for the other heart causes or respiratory illnesses. As in Table 5, there is clear evidence of heterogeneous effects for the two heart-related endpoints.

We tried controlling for the marital status of the mother at birth – which has been shown to be of tremendous importance for childhood health of these cohorts (Bhalotra et al., 2017) – but the coefficient was insignificant and hence it was removed from the final specification displayed in Table 6. We also performed the usual Wald-type tests (see eg. Sec VII.2 of Andersen et al., 1993) of various nested models that excludes quarter-of-birth, mother age-at-birth, father age-at-birth and birth year, respectively. This relies on the standard (non-robust) estimator of the variance-covariance matrix for the Cox model, as elaborated in Fine and Gray (1999). Results are reported in Table 6 by the significance marks at the group-level. We found that the father's

age-at-birth indicators were neither individually nor jointly significant for any cause and hence they are, like marital status, excluded from the final model and the listings in Table 6. Quarter-of-birth is jointly significant for the heart-attack cause, mother age-at-birth for the respiratory illnesses cause and birth year for the heart-attack and other heart disease causes. All at the 0.05-level.

Children born by both younger and older mothers relative to the baseline group experience slightly increased incidence of dying from heart attacks. For respiratory deaths we see the reversed effect where the baseline group has higher heart-attack mortality incidence, while old and young mothers have lower. No effects are observed for the other causes.

Gender displays a rather homogenous reduction in incidence across causes for women, except for GGI cancer where females have a slightly increased incidence. The association for GGI cancer is not observed on the cause-specific fits (see Table 7), which indicates that it is likely an indirect effect on the CIF through genders influence on the other (and residual) causes. However, there is some evidence (Jung et al., 2012) that colorectal and urinary cancers (that account for a large part of the GGI endpoint) show better survival rates in men which in our case would lead to a gender coefficient larger than one. Also, women display better survival for lung cancers (Jung et al., 2012) which also aligns with the results from Table 6.

For quarter-of-birth there is a significant effect on the cumulative incidence for heart-attack only. Interestingly, it appears that birth during the second- or third quarter (warmer periods) increases the incidence of heart-attacks, similar effects are observed for all-cause mortality in Doblhammer and Vaupel (2001). It would be very relevant to investigate whether this is related to the warm gestation interaction result of Bruckner et al. (2014) where the effect of cold acts selectively on those who experienced warm temperatures *in utero*.

For the cancer and heart-attack causes we see that the birth parish frailties are statistically significant. This indicates that cancer and heart-attack mortality is partly influenced by local variations that we are not controlling for. However, while the frailty term is significant, it appears that the addition of frailty does not affect the estimated effects for cold exposure, consult Table A2 in the Appendix.

From the cause-specific estimates, see Table 7, we can obtain relative risk estimates. We see that exposure to temperatures less than -15°C approximately doubles the instantaneous cause-

specific risks for heart-attack and cancer deaths (i.e. during exposure). No effect is found on the cause-specific hazards for death from other heart and respiratory diseases. More precisely, we obtain relative-risk estimates of ≈ 2.3 for cold on the heart-attack hazard. Similarly, we find ≈ 1.8 and ≈ 2.0 for GGI and other cancers, respectively. This is in line with the direction of the effects estimated for the cumulative incidence functions.

The relation between cold temperatures and cardiovascular risk is both supported in the literature (eg. [Donaldson and Keatinge, 1997](#); [Deschenes, 2014](#)), and we also find a very strong non-interacted association between heart-attack deaths and cold exposure. Thus, it is puzzling that no significant (non-interacted) effect of weather is found by [Bruckner et al. \(2014\)](#) even though they apply an exposure indicator similar to ours.

Also, at the 1st percentile threshold, we do not find evidence of a link between cold and respiratory deaths, as has otherwise been suggested (eg. [Donaldson and Keatinge, 1997](#)). However, this changes if we consider a less extreme threshold for the indicator, as we pursue in the following section.

4.5 Threshold, Slack and MCWD Sensitivity

To investigate the impact of the temperature threshold, we re-estimate Specification 2 with a threshold equal to the 5th percentile of the local temperature distribution and with a maximum temperature of $< -5^{\circ}\text{C}$ (compared to $< -15^{\circ}\text{C}$ before). The results are presented in [Table 8](#) and resemble those for the more extreme value of the threshold. However, for the milder temperature exposure we find a significant association between cold and death from respiratory illnesses. It is difficult to assess whether respiratory death is specifically associated with milder (as opposed to extreme) cold weather, or if it is rather a power issue.

Naturally, a less extreme threshold for the temperature results in more and longer periods with cold exposure (i.e. where $Z(t) = 1$). This increases the variation in Z and hence makes it easier to estimate the corresponding coefficient. Heuristically, if we consider the event counts, it is apparent that respiratory deaths (817 events) is lower than deaths from GGI cancer (1239 events) and the heart endpoints (906 + 1169 events). However, it is slightly higher than the number of deaths from other cancers (630 events). We do find a significant effect for other cancer incidence under the 1st percentile threshold even though the number of other cancer

events (640) are lower than that of respiratory deaths (817). This could indicate that the association between respiratory death and cold is weaker compared to that for cold and incidence of death from other cancers. Further investigation of this is required with larger sample sizes to understand whether it is a temperature or power issue.

Table 9 presents the changes in the estimated effect of cold exposure on incidence when we vary the amount of slack. It is clear that the association between heart-attack death and cold is robust across the choice of θ . In addition, we find an effect on the GGI and other cancer cumulative incidences when we increase the slack from 0. Notice also that the estimates are obviously very imprecise for $\theta = 0$ as the absence of slack makes the model rather sensitive to timing in Z and the events.

Finally, while the results are not explicitly presented here, we get cold exposure response patterns similar to Table 6 when we vary the other tuning parameter α which is the number of minimum consecutive wave days (MCWD). Thus, filtering out the shortest cold waves ($\alpha = 1, 2$ or 3 days) does not markedly change the conclusions of Table 6 but the standard errors are larger due to loss of variation in Z .

One of the fundamental assumptions of the Cox regression model and hence (7) is that of proportionality. In particular, we assume that the only part of the hazard that changes due to the passage of time is the baseline. The individual factor is assumed to be purely time-independent. This also means that we assume that the effect of extreme weather exposure is constant over our chosen time scale, i.e. age, so extreme weather affects children, middle aged and old people equally much. As discussed earlier, when the proportionality assumption is violated we can view the estimated effect as a time-averaged effect (Section 5, [Beyersmann et al., 2011](#)). This means that the cold effect could be viewed as an average across all ages, both young and old.

For assessing the proportionality assumption, we inspect the Schoenfeld residual plots (they are not included here, there is one plot per covariate per cause, totaling roughly 60 figures). The Schoenfeld plots provide visual diagnostics and in our case they indicate that there might be violations of the proportionality assumption. However, the usual statistical tests of time-dependence ([Grambsch and Therneau, 1994](#)) cannot reject the null hypothesis of constant hazard ratios at the 0.05-level. Naturally, as the value of a time-varying covariate only matters

at event times, the effect of Z for cause k is driven by observations with event time t where $Z(t) = 1$ which are observed as rather extreme values of the Schoenfeld residuals.

4.6 Competing risks with relative waves and time-varying ratios

Let $Z(t)$ denote the exposure indicator at time t and \mathbf{X} a vector of time-constant covariates. We employ the additive Aalen model for the *all cause* hazard

$$\lambda(t | Z(t), \mathbf{X}) = \lambda_0(t) + \beta\mathbf{X} + \zeta(t)Z(t)$$

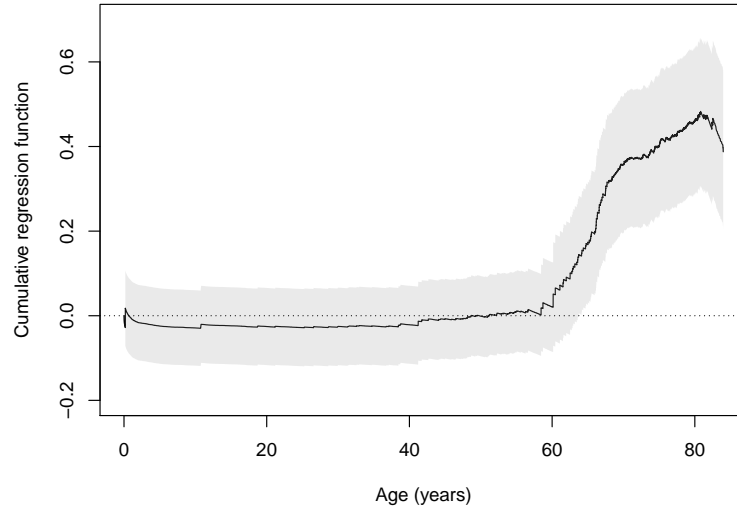
where we assume that the effects of \mathbf{X} are time-independent and parameterized by β while the effect of cold is measured by ζ which is now an arbitrary function of time. Since we are working on the age time-scale this means that the effect of Z (and hence of extreme cold) is allowed to vary across age. The model receives an excellent modern treatment by [Scheike & Martinussen \(2006\)](#). We estimate the cumulative regression function $B(t) = \int_0^t \zeta(s) ds$ by the least-squares estimator as implemented by the `timereg` package in R. Currently, the specification do not account for correlation in survival times within birth parishes.

The alternative specification $\lambda(t | Z(t), \mathbf{X}) = \lambda_0(t) \exp(\beta\mathbf{X} + \zeta(t)Z(t))$ adhering to the usual Cox structure is also possible, but fitting the model is more difficult and somewhat prone to instability compared to the additive version.

The estimated cumulative regression function for Z is depicted in [Figure 7](#). We are concerned with the change in the function as this signifies the underlying effect on the hazard. The signs of the time-dependent effects correspond to the findings from the simpler Cox model where ζ is fixed. The spike around zero is driven by infant mortality, while the slight (but insignificant) dip from around 2 years until 50 years is likely due to a frailty effect where weak individuals are culled at birth leaving “stronger” survivors. The late-life causes primarily occurs from age 45 and onwards which also seems to be the time where the cold effect becomes increasingly pronounced. In particular, we gather that the all-cause effect seen in the time-invariant setting must be driven by the relationship between cold and late-life events.

In addition to the all-cause analysis presented in [Figure 7](#), we have also estimated cause-specific additive hazard models for our set of selected causes, these are presented in [Figure 8](#). The relatively low event-counts (and hence effective sample sizes) makes inference somewhat

Figure 7: Cumulative regression function for Z



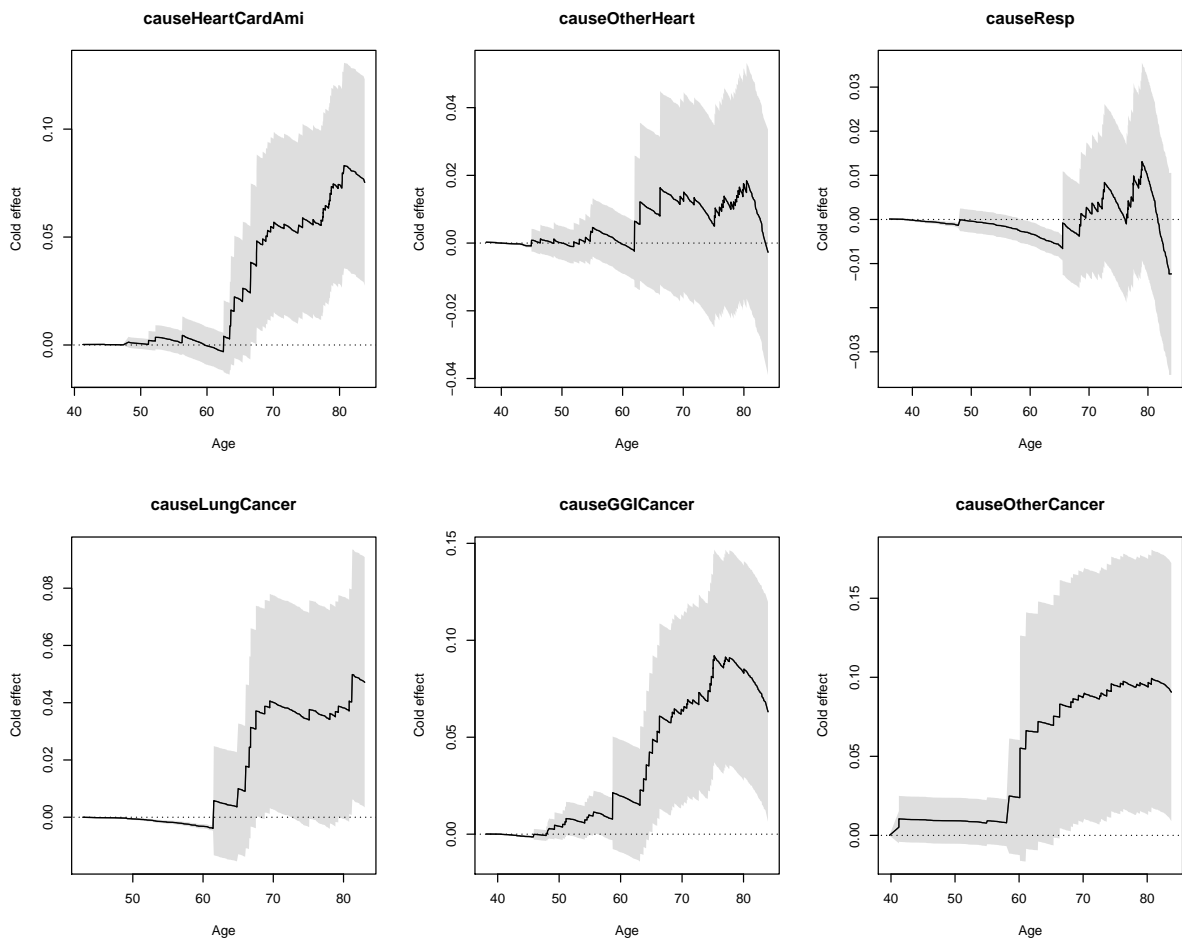
Note: The graph shows the cumulative regression function for Z when modeling the all-cause hazard. The gray area depicts 0.95 confidence bands.

imprecise in the cause-specific setting. However, the estimates of the cumulative regression functions are in general agreement with the results from the Cox approach. It is also possible to estimate the effects on the CIF by the Aalen additive approach, see [Scheike & Martinussen \(2006\)](#).

4.7 Exposure Timing and Harvesting

An interesting question is whether the observed effects of cold on incidence are driven by the first few days after exposure, or whether a prolonged impact exists. In other words, do we, *even after the first k cold days*, still see an effect of cold on mortality in the succeeding time? A crude analysis can be implemented by lagging the weather indicator Z by k days. If the effect of low temperatures is concentrated in the initial days of a wave then we should see smaller effects on the cumulative incidences when we increase k . If, on the other hand, weather displays a prolonged effect (in excess of k days) then the coefficients should stay significantly different from unity even when k is increased considerably.

Figure 8: Cause-specific cumulative regression functions for Z



The cumulative regression function for Z when we model cause-specific additive hazards (Aalen). The gray area depicts pointwise 0.95 confidence bands.

To investigate the dependence on timing of Z relative to event times, we introduce a lagged exposure indicator. There exists more involved approaches to this, eg. proportional lag-exposure models ([Gasparrini, 2014](#)) but we pursue the simpler method here. Let γ be a delay (or lag) parameter and define the lagged exposure indicator process Z_d by

$$Z_d(t) = Z(t - \gamma) \quad (10)$$

where we assume $Z_d(t) = 0$ for $t < \gamma$ even though data could technically be obtained for this interval¹⁷. The model for the subdistribution hazard now becomes

$$\lambda_k(t | \mathbf{X}, Z_d(t)) = \lambda_{0k}(t) \exp(\mathbf{X}\beta_k + \zeta_k Z_d(t)).$$

Considering the ratio of cold days relative to life duration, see [Figure 5](#), we can easily infer that the lag parameter γ has negligible effect on the amount of exposure received, but rather affects the timing of said exposure. However, since we only model a contemporaneous association between cold and mortality, cf. [\(7\)](#), we should see that changes in timing will also affect the estimates considerably.

As discussed in [Deschenes \(2014\)](#), harvesting effects are a common component in the study of temperature and mortality. It is often encountered when investigating sudden exposures, eg. [Schwartz \(2000\)](#). Harvesting refers to the death of fragile individuals, i.e. when an exposure advances death only by a short timespan. Hence, those that die were already on the verge of dying.

The idea is that causes where the mortality response is concentrated right when the cold weather hits exhibits a form of harvesting effects, where many fragile individuals will fail quickly and at a high rate shortly after being exposed. This also means that a lagged exposure would partly filter these immediate effects, and for estimates driven by harvesting we should see that these diminish compared to the reported values in [Table 6](#).

The model in [\(7\)](#) is estimated for Specification 2 from the previous section. [Table 10](#) reports the coefficients for weather exposure only. We vary the delay parameter γ such that the columns in [Table 10](#) correspond to delays of zero, five and ten days. It is seen that the effects of

¹⁷Here $t < \gamma$ corresponds to lags from "exposure" before the individual was born and hence wasn't directly exposed. In-utero exposure is another (and separate) story.

cold exposure on the cumulative incidence functions change when γ is increased. In particular, the effects for the cancer endpoints become insignificant with estimates approaching 1 when cold exposure is lagged 5-10 days. However, the estimate for cold on heart-attack mortality incidence stays significantly different from one and is not lowered much in magnitude. This indicates that the effects for cancer are confined to the first 0-10 days after initial exposure, while the effects for heart-attack lasts longer. This supports an interpretation where the effects on cancer are predominantly driven by immediate harvesting of fragile individuals, while there appears to be a prolonged effect for heart-attack incidence throughout the exposure period.

5 Conclusion

This paper draws on two unique datasets and compares the findings from two distinct modelling approaches. The first dataset contains the universe of death from Sweden between 1968 and 2013 at the county-month level. After generating mortality rates, we employed the standard approach in the economics literature that links these rates in a cross-sectional perspective to average contemporaneous temperature bins.

The second dataset follows a cohort of 30,150 Swedes from 1930 to 2013, from birth until death. We link these lifecycle data to weather data at the daily level to model the impact of cold waves on mortality in a lifecycle perspective. The 2019 cold wave in North America has just drastically illustrated the importance of a better understanding of the consequences of human exposure to extreme cold. Like heat extremes, cold extremes will very likely further increase as a result of climate change (cf. [Peterson et al., 2013](#); [Golledge et al., 2019](#)).

Using the cross-sectional linear, as well as the longitudinal competing risks framework, we consistently find that extreme cold—defined as days with temperatures below the 1st and 5th percentile of the historical local temperature distribution—is significantly linked to higher mortality across a range of causes. In particular, we find that exposure to extreme cold increases the risk of dying from a heart attack. Moreover, we find similar effects for various types of cancer. These findings are robust to modeling migration pattern of humans over their lifecycle and to considering unobserved heterogeneity at the parish level. However, we also find some important qualitative differences between the cross-sectional and longitudinal modeling approaches. For example, while we clearly find a positive link between cold and respiratory

deaths in a longitudinal competing risk design, this link vanishes and even appears negative in the cross-sectional linear modeling approach. One possible reason is that frail individuals with comorbidities might die from heart attacks during cold waves as they dominate the underlying cold-respiratory health effects. This illustrates the need for complementary econometric analyses, such as modeling competing health risks, to better understand how climate change will impact humans over their lifecycle.

As more lifecycle data will become available, researchers will be increasingly able to track humans over their lifecycle. Applications to more regions and cohorts will enhance our understanding of the complex interplay between ambient temperature exposure, human adaptation, and health. Refinements in measuring exposure and refinements in statistical modeling will contribute to a better understanding of how climate change affects human health in the long-run.

References

- Aalen, O., O. Borgan, and H. Gjessing (2008). *Survival and event history analysis: a process point of view*. Springer.
- Almond, D. and J. Currie (2011). Killing me softly: The Fetal Origins Hypothesis. *Journal of Economic Perspectives* 25(3), 153–172.
- Andersen, P. K., O. Borgan, R. D. Gill, and N. Keiding (1993). *Statistical models based on counting processes*. Springer.
- Andersen, P. K. and N. Keiding (2012). Interpretability and importance of functionals in competing risks and multistate models. *Statistics in medicine* 31(11-12), 1074–1088.
- Barreca, A., K. Clay, O. Deschênes, M. Greenstone, and J. S. Shapiro (2016). Adapting to climate change: The remarkable decline in the U.S. temperature-mortality relationship over the 20th century. *Journal of Political Economy* 124(1), 105–159.
- Beyersmann, J., A. Allignol, and M. Schumacher (2011). *Competing risks and multistate models with R*. Springer Science & Business Media.
- Bhalotra, S., M. Karlsson, and T. Nilsson (2017). Infant health and longevity: Evidence from a historical intervention in Sweden. *Journal of the European Economic Association* 15(5), 1101–1157.
- Bruckner, T. A., G. J. van den Berg, K. R. Smith, and R. A. Catalano (2014). Ambient temperature during gestation and cold-related adult mortality in a Swedish cohort, 19152002. *Social Science & Medicine* 119, 191 – 197.
- Cortese, G. and P. K. Andersen (2010). Competing risks and time-dependent covariates. *Biometrical Journal* 52(1), 138–158.
- Cox, D. R. (1972). Regression models and life-tables. *Journal of the Royal Statistical Society. Series B (Methodological)* 34(2), 187–220.
- Currie, J., J. S. G. Zivin, J. Mullins, and M. J. Neidell (2014). What do we know about short and long term effects of early life exposure to pollution? *Annual Review of Resource Economics* 6, 217–247.
- Curriero, F. C., K. S. Heiner, J. M. Samet, S. L. Zeger, L. Strug, and J. A. Patz (2002). Temperature and mortality in 11 cities of the Eastern United States. *American Journal of Epidemiology* 155(1), 80–87.
- Deschenes, O. (2014). Temperature, human health, and adaptation: A review of the empirical literature. *Energy Economics* 46, 606 – 619.
- Deschênes, O. and M. Greenstone (2011). Climate change, mortality, and adaptation: Evidence from annual fluctuations in weather in the U.S. *American Economic Journal: Applied Economics* 3(4), 152–85.
- Deschênes, O. and E. Moretti (2009). Extreme weather events, mortality and migration. *The Review of Economics and Statistics* 91(4), 659–681.
- Doblhammer, G. and J. Vaupel (2001, February). Lifespan depends on month of birth. *Proceedings of the National Academy of Sciences of the United States of America* 98(5), 29342939.

- Dockery, D. W., C. A. Pope, X. Xu, J. D. Spengler, J. H. Ware, M. E. Fay, B. G. J. Ferris, and F. E. Speizer (1993). An association between air pollution and mortality in six U.S. cities. *New England Journal of Medicine* 329(24), 1753–1759.
- Donaldson, G. C. and W. R. Keatinge (1997). Early increases in ischaemic heart disease mortality dissociated from and later changes associated with respiratory mortality after cold weather in south east England. *Journal of Epidemiology and Community Health* (1979-) 51(6), 643–648.
- Fine, J. P. and R. J. Gray (1999). A proportional hazards model for the subdistribution of a competing risk. *Journal of the American statistical association* 94(446), 496–509.
- Gasparrini, A. (2014). Modeling exposure–lag–response associations with distributed lag non-linear models. *Statistics in medicine* 33(5), 881–899.
- Golledge, N. R., E. D. Keller, N. Gomez, K. A. Naughten, J. Bernales, L. D. Trusel, and T. L. Edwar (2019). Global environmental consequences of twenty-first-century ice-sheet melt. *Nature* 566(20), 65–72.
- Graff Zivin, J., S. M. Hsiang, and M. Neidell (2018). Temperature and human capital in the short and long run. *Journal of the Association of Environmental and Resource Economists* 5(1), 77–105.
- Grambsch, P. M. and T. M. Therneau (1994). Proportional hazards tests and diagnostics based on weighted residuals. *Biometrika* 81(3), 515–526.
- Graw, F., T. A. Gerds, and M. Schumacher (2009). On pseudo-values for regression analysis in competing risks models. *Lifetime Data Analysis* 15(2), 241–255.
- Gray, R. J. (1988). A class of k-sample tests for comparing the cumulative incidence of a competing risk. *The Annals of statistics* 16(3), 1141–1154.
- Grossman, M. (1972). On the concept of health capital and the demand for health. *Journal of Political Economy* 80(2), 223–255.
- Heckley, G., M. Fischer, U.-G. Gerdtham, M. Karlsson, G. Kjellsson, and T. Nilsson (2018). The long-term impact of education on mortality and health: Evidence from Sweden. Working Paper 2018:8, Lund University, Department of Economics.
- Jung, K.-W., S. Park, A. Shin, C.-M. Oh, H.-J. Kong, J. K. Jun, and Y.-J. Won (2012). Do female cancer patients display better survival rates compared with males? analysis of the Korean national registry data, 2005–2009. *PLOS ONE* 7(12), 1–6.
- Kalbfleisch, J. D. and R. L. Prentice (2011). *The statistical analysis of failure time data*, Volume 360. John Wiley & Sons.
- Karlsson, M. and N. R. Ziebarth (2018). Population health effects and health-related costs of extreme temperatures: Comprehensive evidence from Germany. *Journal of Environmental Economics and Management* 91(-), 93–117.
- Lancaster, T. (1992). *The econometric analysis of transition data*. Econometric Society Monographs. Cambridge University Press.
- Latouche, A., R. Porcher, and S. Chevret (2005). A note on including time-dependent covariate in regression model for competing risks data. *Biometrical journal* 47(6), 807–814.

- Lepeule, J., V. Rondeau, L. Filleul, and J.-F. Dartigues (2006). Survival analysis to estimate association between short-term mortality and air pollution. *Environmental health perspectives* 114(2), 242.
- Martinussen, T. and T. H. Scheike (2006). *Dynamic regression models for survival data*. Springer.
- Medina-Ramón, M. and J. Schwartz (2007). Temperature, temperature extremes, and mortality: a study of acclimatisation and effect modification in 50 us cities. *Occupational and environmental medicine* 64(12), 827–833.
- Peterson, T. C., R. R. Heim, R. Hirsch, D. P. Kaiser, H. Brooks, N. S. Diffenbaugh, R. M. Dole, J. P. Giovannetone, K. Guirguis, T. R. Karl, R. W. Katz, K. Kunkel, D. Lettenmaier, G. J. McCabe, C. J. Paciorek, K. R. Ryberg, S. Schubert, V. B. S. Silva, B. C. Stewart, A. V. Vecchia, G. Villarini, R. S. Vose, J. Walsh, M. Wehner, D. Wolock, K. Wolter, C. A. Woodhouse, and D. Wuebbles (2013). Monitoring and understanding changes in heat waves, cold waves, floods, and droughts in the United States: State of knowledge. *Bulletin of the American Meteorological Society* 94(6), 821–834.
- R Core Team (2016). *R: A Language and Environment for Statistical Computing*. Vienna, Austria: R Foundation for Statistical Computing.
- Ripatti, S. and J. Palmgren (2004). Estimation of multivariate frailty models using penalized partial likelihood. *Biometrics* 56(4), 1016–1022.
- Scheike, T. H. and M.-J. Zhang (2008). Flexible competing risks regression modeling and goodness-of-fit. *Lifetime data analysis* 14(4), 464.
- Schwartz, J. (2000). Harvesting and long term exposure effects in the relation between air pollution and mortality. *American journal of epidemiology* 151(5), 440–448.
- Son, J.-Y., N. Gouveia, M. A. Bravo, C. U. de Freitas, and M. L. Bell (2016). The impact of temperature on mortality in a subtropical city: Effects of cold, heat, and heat waves in São Paulo, Brazil. *International Journal of Biometeorology* 60(1), 113–121.
- Therneau, T. M. (2015). *A Package for Survival Analysis in S*. version 2.38.
- van den Berg, G. J., G. Doblhammer, and K. Christensen (2009). Exogenous determinants of early-life conditions, and mortality later in life. *Social Science & Medicine* 68(9), 1591–1598.
- van den Berg, G. J., G. Doblhammer-Reiter, and K. Christensen (2011). Being born under adverse economic conditions leads to a higher cardiovascular mortality rate later in life: Evidence based on individuals born at different stages of the business cycle. *Demography* 48(2), 507–530.
- van den Berg, G. J., M. Lindeboom, and F. Portrait (2006). Economic conditions early in life and individual mortality. *American Economic Review* 96(1), 290–302.
- van den Berg, G. J., M. Lindeboom, and F. Portrait (2011). Conjugal bereavement effects on health and mortality at advanced ages. *Journal of Health Economics* 30(4), 774 – 794.
- Wilde, J., B. H. Apouey, and T. Jung (2017). The effect of ambient temperature shocks during conception and early pregnancy on later life outcomes. *European Economic Review* 97(Supplement C), 87 – 107.
- Yeung, G. Y. C., G. J. van den Berg, M. Lindeboom, and F. R. M. Portrait (2014). The impact of early-life economic conditions on cause-specific mortality during adulthood. *Journal of Population Economics* 27(3), 895–919.

Zhou, B., A. Latouche, V. Rocha, and J. Fine (2010). Competing risks regression for stratified data. *Biometrics* 67(2), 661–670.

Zivin, J. G. and J. Shrader (2016). Temperature extremes, health, and human capital. *The Future of Children* 26(1), 31–50.

Table 1: Descriptive statistics

VARIABLE:	MEAN	SD	Min	Max	N
Heart attack	1.775	3.38	0.00	46.78	12,384
Other heart	6.741	7.09	0.00	82.63	12,384
Respiratory disease	0.570	1.09	0.00	28.88	12,384
Lung cancer	0.621	1.27	0.00	27.33	12,384
GGI cancers	1.771	2.58	0.00	43.14	12,384
Other cancers	5.825	6.41	0.00	70.19	12,384
Other	15.174	15.97	0.37	149.89	12,384
All causes	32.478	31.95	0.65	285.14	12,384

Source: SIP. Own calculations. This table shows county-month mortality rates by cause of death from 1968 to 2012. Over this time period, the number of counties in Sweden varied between 21 and 25.

Table 2: Summary Statistics: Events by Cause of Death

Event	Frequency	Proportion
Heart-attack (acute myocardial infarction)	936	0.071
Other heart diseases (excluding cardiac arrest and heart attack)	1,202	0.091
Respiratory diseases	853	0.065
Lung cancers	447	0.034
Genital and gastrointestinal (GGI) cancers	1,280	0.097
Other cancers	650	0.049
Other	7,781	0.592
All-causes	13,149	
Administratively censored at 2013-12-31	16,997	
Total	30,146	

The table shows the number of events (deaths) separately for each cause of death, along with its share out of the total number of deaths. The table also shows the number of "administratively censored" individuals, i.e., individuals who have not died by December 31st, 2013.

Table 3: Linear Cross-Sectional Mortality Rate Model

	All-cause	AMI	Other Heart	Respiratory	Lung cancer	GGI	Other canc.
PERCENTILE 1, SLACK 0							
cv10	0.2002 (0.205)	0.0652 (0.044)	0.2421 (0.127)	-0.0350 (0.044)	0.0193 (0.023)	-0.0114 (0.031)	0.0113 (0.074)
PERCENTILE 1, SLACK 10							
cv110	0.0857 (0.064)	0.0150 (0.009)	0.0240 (0.028)	-0.0114 (0.010)	0.0048 (0.005)	-0.0075 (0.006)	0.0098 (0.020)
PERCENTILE 5, SLACK 0							
cv50	0.3148*** (0.078)	0.0442* (0.021)	0.1067** (0.032)	-0.0144 (0.015)	0.0162 (0.010)	-0.0073 (0.011)	0.0565 (0.031)
PERCENTILE 5, SLACK 10							
cv510	0.1956** (0.054)	0.0246* (0.010)	0.0214* (0.009)	-0.0063 (0.006)	0.0086 (0.004)	-0.0108 (0.005)	0.0292* (0.014)
Baseline	31.37	1.71	6.53	0.55	0.59	1.69	5.57
R2	0.90	0.62	0.86	0.57	0.59	0.69	0.79
N	12,384	12,384	12,384	12,384	12,384	12,384	12,384
County FE	X	X	X	X	X	X	X
Year × Month FE	X	X	X	X	X	X	X

Source: SIP from 1968 to 2012. Own calculations. This shows results from a model similar to Equation (1). Outcome variable is the mortality rates at the county-month level from 1968 to 2012. Over this time period, the number of counties in Sweden varied between 21 and 25.

Table 4: Lifecycle Competing Risk Model—Effects on All-Cause Mortality, Specification 2

Specification 2	
Cold weather, Z	1.531 (***) [1.375; 1.706]
Female	0.986 (***) [0.981; 0.991]
Twin	1.221 (***) [1.102; 1.352]
Quarter of birth	
- Second	1.012 [0.964; 1.062]
- Third	1.005 [0.957; 1.055]
- Fourth	1.007 [0.957; 1.059]
Birth year	
- 1931	0.973 [0.922; 1.027]
- 1932	0.918 (**) [0.868; 0.971]
- 1933	0.874 (***) [0.825; 0.927]
- 1934	0.855 (***) [0.806; 0.908]
Mother age	
- Young, < 25.8	1.048 (*) [1.004; 1.093]
- Old, > 32.2	1.038 (.) [0.995; 1.083]
Parish frailty	- (***)

The estimated effects on the all-cause hazard. The number of minimum consecutive wave days (α) is zero, slack (θ) is 10 days and the indicator delay (γ) is 0. The p-values are based on the non-robust¹⁴ standard errors for the *transformed* coefficients and (**): < 0.001, (*): < 0.01, (*) < 0.05, (.) < 0.1.

Table 5: Lifecycle Competing Risk Model—Effects on Cumulative Incidence, Specification 1

	Heart-attack	Other heart	Respiratory	Lung cancer	GGI cancer	Other cancer
Cold weather, Z	2.080 (***) [1.500; 2.883]	1.079 [0.750; 1.552]	1.083 [0.701; 1.672]	1.553 [0.910; 2.650]	1.587 (**) [1.165; 2.162]	1.689 (*) [1.112; 2.565]
Female	0.414 (***) [0.358; 0.479]	0.485 (***) [0.429; 0.549]	0.653 (***) [0.567; 0.752]	0.754 (**) [0.622; 0.913]	1.172 (**) [1.049; 1.310]	0.896 [0.766; 1.048]
Events	906	1169	817	431	1239	630

Estimates originate from the subdistribution hazard models for the selected causes. The number of minimum consecutive wave days α is in all cases zero, slack θ is 10 days and the indicator delay γ is 0. The temperature threshold is the local 1st percentile with a minimum temperature limit of < -15°C . The 0.95-confidence intervals and the significance marks are based on the non-robust standard errors for the *transformed* coefficients and (**): < 0.001, (*): < 0.01, (*) < 0.05, (.) < 0.1.

Table 6: Lifecycle Competing Risk Model—Effects on Cumulative Incidence, Specification 2

	Heart-attack	Other heart	Respiratory	Lung cancer	GGI cancer	Other cancer
Cold weather, Z	2.024 (***) [1.458; 2.810]	1.075 [0.747; 1.546]	1.085 [0.703; 1.675]	1.682 (.) [0.983; 2.877]	1.608 (**) [1.179; 2.193]	1.787 (**) [1.174; 2.719]
Female	0.414 (***) [0.358; 0.478]	0.484 (***) [0.428; 0.548]	0.654 (***) [0.568; 0.753]	0.756 (**) [0.624; 0.916]	1.173 (**) [1.049; 1.312]	0.895 [0.765; 1.047]
Twin	0.516 (*) [0.298; 0.893]	0.900 [0.623; 1.302]	0.939 [0.608; 1.448]	0.850 [0.453; 1.592]	1.113 [0.802; 1.545]	1.036 [0.648; 1.658]
Quarter of birth	(**)					
- Second	1.241 (*) [1.034; 1.488]	1.104 [0.942; 1.293]	0.892 [0.738; 1.079]	1.121 [0.854; 1.472]	1.026 [0.880; 1.197]	0.930 [0.750; 1.155]
- Third	1.234 (*) [1.028; 1.483]	0.996 [0.846; 1.173]	1.000 [0.829; 1.205]	1.143 [0.871; 1.502]	0.948 [0.810; 1.110]	1.002 [0.809; 1.241]
- Fourth	0.940 [0.769; 1.150]	1.021 [0.864; 1.206]	0.877 [0.718; 1.071]	1.267 (.) [0.965; 1.665]	0.994 [0.847; 1.167]	0.872 [0.694; 1.096]
Birth year	(***)	(*)				
- 1931	0.990 [0.822; 1.193]	0.898 [0.760; 1.062]	1.085 [0.888; 1.326]	1.102 [0.826; 1.470]	0.948 [0.802; 1.121]	0.969 [0.760; 1.234]
- 1932	0.913 [0.753; 1.106]	0.874 [0.736; 1.039]	1.017 [0.824; 1.257]	1.300 (.) [0.982; 1.721]	0.949 [0.800; 1.126]	0.984 [0.770; 1.256]
- 1933	0.715 (**) [0.578; 0.886]	0.908 [0.760; 1.085]	1.018 [0.814; 1.274]	0.933 [0.680; 1.278]	0.872 [0.727; 1.044]	1.086 [0.849; 1.389]
- 1934	0.691 (**) [0.556; 0.860]	0.712 (**) [0.586; 0.864]	0.955 [0.756; 1.206]	0.925 [0.673; 1.272]	1.004 [0.842; 1.199]	1.058 [0.822; 1.362]
Mother age			(*)			
- Young, < 25.8	1.147 (.) [0.977; 1.347]	0.895 [0.777; 1.032]	0.868 (.) [0.736; 1.024]	0.952 [0.759; 1.195]	1.002 [0.876; 1.147]	1.056 [0.874; 1.276]
- Old, > 32.2	1.129 [0.963; 1.324]	0.987 [0.861; 1.131]	0.812 (*) [0.688; 0.959]	0.899 [0.714; 1.133]	0.924 [0.806; 1.058]	0.993 [0.820; 1.202]
Parish frailty	- (*)	-	-	- (*)	- (*)	- (*)
Events	906	1169	817	431	1239	630

Estimates originate from the subdistribution hazard models for the selected causes. The number of minimum consecutive wave days α is in all cases zero, slack θ is 10 days and the indicator delay γ is 0. The temperature threshold is the local 1st percentile with a minimum temperature limit of $< -15^{\circ}\text{C}$. The 0.95-confidence intervals and the significance marks are based on the non-robust standard errors for the *transformed* coefficients and (**): < 0.001 , (**): < 0.01 , (*) < 0.05 , (.) < 0.1 .

Table 7: Lifecycle Competing Risk Model—Effects on Cause-Specific Hazards, Specification 2

	Heart-attack	Other heart	Respiratory	Lung cancer	GGI cancer	Other cancer
Cold weather, Z	2.317 (***) [1.668; 3.219]	1.200 [0.834; 1.726]	1.192 [0.771; 1.842]	1.884 (*) [1.101; 3.224]	1.787 (***) [1.310; 2.438]	1.969 (**) [1.294; 2.997]
Female	0.359 (***) [0.310; 0.415]	0.419 (***) [0.370; 0.474]	0.543 (***) [0.471; 0.625]	0.646 (***) [0.534; 0.783]	0.994 [0.889; 1.111]	0.761 (**) [0.650; 0.890]
Twin	0.562 (*) [0.325; 0.973]	0.976 [0.675; 1.412]	1.019 [0.660; 1.573]	0.931 [0.497; 1.745]	1.224 [0.882; 1.699]	1.140 [0.713; 1.823]
Quarter of birth						
- Second	1.243 (*) [1.036; 1.491]	1.105 [0.943; 1.295]	0.900 [0.744; 1.089]	1.128 [0.859; 1.480]	1.030 [0.883; 1.201]	0.937 [0.755; 1.163]
- Third	1.237 (*) [1.030; 1.486]	1.002 [0.851; 1.179]	1.003 [0.832; 1.209]	1.146 [0.873; 1.506]	0.950 [0.811; 1.112]	1.004 [0.811; 1.244]
- Fourth	0.945 [0.773; 1.155]	1.023 [0.866; 1.209]	0.883 [0.723; 1.079]	1.270 (.) [0.967; 1.669]	1.002 [0.854; 1.176]	0.878 [0.699; 1.103]
Birth year						
- 1931	0.970 [0.805; 1.168]	0.887 [0.750; 1.048]	1.061 [0.868; 1.296]	1.083 [0.812; 1.444]	0.937 [0.793; 1.108]	0.953 [0.748; 1.213]
- 1932	0.891 [0.735; 1.080]	0.851 (.) [0.716; 1.011]	0.982 [0.795; 1.213]	1.268 (.) [0.958; 1.678]	0.927 [0.781; 1.099]	0.962 [0.753; 1.228]
- 1933	0.689 (**) [0.557; 0.853]	0.874 [0.731; 1.044]	0.972 [0.777; 1.216]	0.900 [0.656; 1.233]	0.846 (.) [0.706; 1.014]	1.047 [0.818; 1.339]
- 1934	0.655 (***) [0.527; 0.814]	0.677 (***) [0.557; 0.823]	0.896 [0.709; 1.132]	0.882 [0.641; 1.213]	0.959 [0.803; 1.144]	1.005 [0.781; 1.294]
Mother age						
- Young, < 25.8	1.179 (*) [1.005; 1.385]	0.924 [0.802; 1.065]	0.898 [0.761; 1.059]	0.980 [0.781; 1.230]	1.030 [0.900; 1.179]	1.085 [0.897; 1.311]
- Old, > 32.2	1.153 (.) [0.983; 1.352]	1.014 [0.885; 1.162]	0.840 (*) [0.711; 0.992]	0.920 [0.731; 1.159]	0.950 [0.829; 1.088]	1.015 [0.839; 1.229]
Parish frailty	- (*)	-	-	- (*)	- (*)	- (.)
Events	906	1169	817	431	1239	630

Estimates originate from the subdistribution hazard models for the selected causes. The number of minimum consecutive wave days α is in all cases zero, slack θ is 10 days and the indicator delay γ is 0. The temperature threshold is the local 1st percentile with a minimum temperature limit of $< -15^\circ\text{C}$. The 0.95-confidence intervals and the significance marks are based on the non-robust standard errors for the *transformed* coefficients and (**): < 0.001 , (**): < 0.01 , (*) < 0.05 , (.) < 0.1 .

Table 8: Lifecycle Competing Risk Model—Effects on Cumulative Incidence, Specification 2, 5th Percentile Threshold

	Heart-attack	Other heart	Respiratory	Lung cancer	GGI cancer	Other cancer
Cold weather, Z	2.009 (***) [1.590; 2.538]	1.090 [0.850; 1.397]	1.276 (.) [0.969; 1.680]	1.453 (.) [0.987; 2.139]	1.408 (**) [1.123; 1.764]	1.647 (**) [1.224; 2.218]
Female	0.414 (***) [0.358; 0.478]	0.484 (***) [0.428; 0.548]	0.654 (***) [0.568; 0.753]	0.756 (**) [0.624; 0.916]	1.173 (**) [1.049; 1.312]	0.895 [0.765; 1.047]
Twin	0.515 (*) [0.298; 0.891]	0.900 [0.622; 1.302]	0.939 [0.608; 1.448]	0.849 [0.453; 1.591]	1.112 [0.801; 1.544]	1.036 [0.648; 1.657]
Quarter of birth						
- Second	1.241 (*) [1.034; 1.489]	1.104 [0.942; 1.293]	0.892 [0.737; 1.078]	1.121 [0.854; 1.472]	1.027 [0.881; 1.198]	0.931 [0.750; 1.155]
- Third	1.232 (*) [1.026; 1.480]	0.997 [0.847; 1.173]	0.998 [0.828; 1.203]	1.144 [0.871; 1.503]	0.949 [0.810; 1.111]	1.004 [0.811; 1.244]
- Fourth	0.937 [0.766; 1.146]	1.021 [0.864; 1.206]	0.877 [0.718; 1.071]	1.267 (.) [0.964; 1.665]	0.995 [0.848; 1.168]	0.873 [0.695; 1.097]
Birth year						
- 1931	0.990 [0.822; 1.193]	0.898 [0.760; 1.062]	1.085 [0.888; 1.326]	1.102 [0.826; 1.470]	0.948 [0.802; 1.121]	0.969 [0.761; 1.235]
- 1932	0.913 [0.753; 1.107]	0.874 [0.736; 1.039]	1.018 [0.824; 1.257]	1.298 (.) [0.981; 1.718]	0.949 [0.800; 1.126]	0.983 [0.770; 1.254]
- 1933	0.716 (**) [0.578; 0.886]	0.908 [0.760; 1.085]	1.018 [0.814; 1.273]	0.931 [0.680; 1.277]	0.871 [0.727; 1.044]	1.085 [0.848; 1.387]
- 1934	0.691 (**) [0.556; 0.859]	0.711 (**) [0.586; 0.864]	0.954 [0.755; 1.205]	0.924 [0.672; 1.271]	1.003 [0.841; 1.198]	1.057 [0.821; 1.360]
Mother age						
- Young, < 25.8	1.147 (.) [0.977; 1.346]	0.895 [0.777; 1.032]	0.868 (.) [0.736; 1.024]	0.952 [0.759; 1.195]	1.002 [0.876; 1.147]	1.056 [0.873; 1.276]
- Old, > 32.2	1.128 [0.962; 1.324]	0.987 [0.861; 1.131]	0.812 (*) [0.687; 0.958]	0.899 [0.714; 1.133]	0.923 [0.806; 1.058]	0.993 [0.820; 1.202]
Parish frailty	- (*)	-	-	- (*)	- (*)	- (*)
Events	906	1169	817	431	1239	630

Estimates originate from the subdistribution hazard models for the selected causes. The number of minimum consecutive wave days α is in all cases two, slack θ is 10 days and the indicator delay γ is 0. The temperature threshold is the local 5th percentile with a minimum temperature limit of $< -5^\circ\text{C}$. The 0.95-confidence intervals and the significance marks are based on the non-robust standard errors for the *transformed* coefficients and (**): < 0.001 , (**): < 0.01 , (*) < 0.05 , (.) < 0.1 .

Table 9: Lifecycle Competing Risk Model—Cumulative Incidence with Varying Indicator Slack θ

	$\theta = 0$ days	$\theta = 5$ days	$\theta = 10$ days
Heart-attack	2.863 (**) [1.481; 5.534]	1.820 (**) [1.165; 2.844]	2.117 (***) [1.511; 2.966]
Other heart	0.422 [0.105; 1.691]	0.732 [0.414; 1.294]	1.014 [0.687; 1.498]
Respiratory	1.561 [0.647; 3.763]	1.227 [0.722; 2.084]	1.045 [0.662; 1.650]
Lung cancer	2.092 [0.670; 6.530]	1.793 (.) [0.923; 3.484]	1.516 [0.850; 2.704]
GGI cancer	1.565 [0.744; 3.295]	1.410 [0.923; 2.154]	1.560 (**) [1.126; 2.161]
Other cancer	1.351 [0.434; 4.209]	1.804 (*) [1.059; 3.075]	1.727 (*) [1.113; 2.679]

Estimates originate from the subdistribution hazard models for the selected causes and are displayed on the exponential scale. The number of minimum consecutive wave days α is in all cases zero, delay γ is 0 days and the results are displayed for three different values of indicator slack θ . The temperature threshold is set to the individualized 1st percentile with a minimum of -15°C . The confidence intervals are based on the non-robust¹⁵ standard errors for the transformed coefficients. The statistical significance is displayed according to (**): < 0.001 , (**): < 0.01 , (*) < 0.05 , (.) < 0.1 .

Table 10: Lifecycle Competing Risk Model—Cumulative Incidence with Varying Indicator Delay γ

	$\gamma = 0$ days	$\gamma = 5$ days	$\gamma = 10$ days
Heart-attack	2.117 (***) [1.511; 2.966]	1.805 (**) [1.257; 2.593]	1.984 (**) [1.403; 2.806]
Other heart	1.014 [0.687; 1.498]	1.215 [0.849; 1.739]	1.294 [0.914; 1.833]
Respiratory	1.045 [0.662; 1.650]	1.101 [0.706; 1.719]	1.100 [0.705; 1.717]
Lung cancer	1.516 [0.850; 2.704]	1.520 [0.852; 2.710]	1.388 [0.759; 2.536]
GGI cancer	1.560 (**) [1.126; 2.161]	1.387 (.) [0.984; 1.955]	1.091 [0.743; 1.601]
Other cancer	1.727 (*) [1.113; 2.679]	1.299 [0.788; 2.142]	0.880 [0.483; 1.602]

Estimates originate from the subdistribution hazard models for the selected causes and are displayed on the exponential scale. The number of minimum consecutive wave days α is in all cases zero, slack θ is 10 days and the results are displayed for four different values of indicator delay γ . The temperature threshold is set to the individualized 1st percentile with a minimum of -15°C . The confidence intervals are based on the non-robust¹⁶ standard errors for the transformed coefficients. The statistical significance is displayed according to (**): < 0.001 , (**): < 0.01 , (*) < 0.05 , (.) < 0.1 .

Appendix

A1 Code

All computational work has been done in R and C++. The rather extensive scripts are available upon request.

A2 Results without Frailty

Table A2: Effects on cumulative incidence are shown; Specification 2 without frailty

	Heart-Attack	Other Heart	Respiratory	Lung Cancer	GGI Cancer	Other Cancer
Cold weather, Z	2.070 (***) [1.493; 2.871]	1.075 [0.747; 1.546]	1.085 [0.703; 1.675]	1.546 [0.906; 2.640]	1.588 (**) [1.165; 2.162]	1.687 (*) [1.111; 2.564]
Female	0.414 (***) [0.359; 0.479]	0.484 (***) [0.428; 0.548]	0.654 (***) [0.568; 0.753]	0.756 (**) [0.624; 0.916]	1.174 (**) [1.050; 1.313]	0.895 [0.765; 1.047]
Twin	0.515 (*) [0.298; 0.891]	0.900 [0.623; 1.302]	0.939 [0.608; 1.448]	0.849 [0.453; 1.591]	1.100 [0.793; 1.526]	1.055 [0.660; 1.686]
Quarter of birth						
- Second	1.242 (*) [1.036; 1.490]	1.104 [0.942; 1.293]	0.892 [0.738; 1.079]	1.125 [0.857; 1.477]	1.027 [0.880; 1.197]	0.933 [0.752; 1.159]
- Third	1.235 (*) [1.028; 1.483]	0.996 [0.846; 1.173]	1.000 [0.829; 1.205]	1.144 [0.871; 1.503]	0.948 [0.810; 1.110]	1.002 [0.809; 1.241]
- Fourth	0.936 [0.766; 1.145]	1.021 [0.864; 1.206]	0.877 [0.718; 1.071]	1.270 (.) [0.967; 1.668]	0.994 [0.846; 1.166]	0.873 [0.695; 1.097]
Birth year						
- 1931	0.992 [0.824; 1.195]	0.898 [0.760; 1.062]	1.085 [0.888; 1.326]	1.090 [0.818; 1.454]	0.943 [0.798; 1.115]	0.967 [0.760; 1.232]
- 1932	0.912 [0.752; 1.105]	0.874 [0.736; 1.039]	1.017 [0.824; 1.257]	1.305 (.) [0.986; 1.728]	0.947 [0.799; 1.124]	0.987 [0.773; 1.260]
- 1933	0.716 (**) [0.578; 0.886]	0.908 [0.760; 1.085]	1.018 [0.814; 1.273]	0.937 [0.684; 1.284]	0.872 [0.728; 1.045]	1.093 [0.855; 1.398]
- 1934	0.692 (**) [0.557; 0.860]	0.712 (**) [0.586; 0.864]	0.955 [0.756; 1.206]	0.932 [0.677; 1.281]	1.002 [0.840; 1.196]	1.064 [0.827; 1.369]
Mother age						
- Young, < 25.8	1.146 (.) [0.976; 1.345]	0.895 [0.777; 1.032]	0.868 (.) [0.736; 1.024]	0.956 [0.762; 1.200]	1.007 [0.880; 1.151]	1.055 [0.873; 1.275]
- Old, > 32.2	1.138 [0.970; 1.334]	0.987 [0.861; 1.131]	0.812 (*) [0.688; 0.959]	0.874 [0.694; 1.100]	0.916 [0.800; 1.049]	0.978 [0.808; 1.183]
Events	906	1169	817	431	1239	630

The estimates originate from the subdistributional hazard models for the selected causes. In all cases, the number of minimum consecutive wave days, α , is zero; slack, θ , is 10 days and the indicator delay, γ , is 0. The temperature threshold is the 1st percentile of the local temperature distribution with a minimum temperature threshold of $< -15^\circ\text{C}$. The 95%-confidence intervals and statistical significance are based on the non-robust standard errors for the *transformed* coefficients. (**): < 0.01 , (*): < 0.05 , (.) < 0.1 .

A3 Categorization of Cause-of-Deaths

Table A3: Overview of the ICD groupings.

Cause	<i>n</i>
Heart-Attack (AMI)	936
- Acute myocardial infarction	936
Other Heart-Disease	1280
- Heart failure	470
- Other forms of heart disease	124
- Chronic ischaemic heart disease	117
- Acute pulmonary heart disease	95
- Other cardiac arrhythmias	58
- Complications and ill-defined descriptions of heart disease	36
- Essential hypertension	12
- "Rare" cases (less than 10 occurrences)	139
Respiratory Disease	853
- Pneumonia, organism unspecified	387
- Respiratory failure	118
- Pulmonary oedema	81
- Other chronic obstructive pulmonary disease	66
- Other chronic obstructive pulmonary disease	66
- Pneumonitis due to solids and liquids	39
- Bronchopneumonia, organism unspecified	29
- Pulmonary congestion and hypostasis	16
- "Rare" cases (less than 10 occurrences)	51
Lung Cancer	447
- Malignant neoplasm of trachea, bronchus and lung	396
- "Rare" cases (less than 10)	51
GGI Cancer	1280
- Malignant neoplasm of prostate	186
- Malignant neoplasm of pancreas	184
- Malignant neoplasm of colon	180
- Malignant neoplasm of breast	159
- Malignant neoplasm of ovary	100
- Malignant neoplasm of rectum	97
- Malignant neoplasm of stomach	97
- Malignant neoplasm of liver	76
- Malignant neoplasm of kidney and urinary	31
- Malignant neoplasm of digestive organs	21
- Malignant neoplasm of cervix	10
- "Rare" cases (less than 10 occurrences)	139
Other cancer	652
- Malignant neoplasm of brain	69
- Multiple myeloma and malignant plasma cell neoplasms	35
- Malignant neoplasm of bladder	34
- Malignant neoplasm without specification of site	41
- Melanoma and other malignant neoplasms of skin	26
- Myeloid leukaemia	22
- Secondary malignant neoplasm of respiratory and digestive organs	37
- Other and unspecified types of non-Hodgkin's lymphoma	25
- Secondary malignant neoplasm of other sites	38
- Malignant neoplasm of other and ill-defined sites	26
- Malignant neoplasms of mesothelial and soft tissue	19
- Diffuse non-Hodgkin's lymphoma	11
- Other malignant neoplasm of lymphoid and histiocytic tissue	13
- "Rare" cases (less than 10)	256
The underlying ICD codes for each of our coarser groups. Rare cases covers all ICD codes with less than 10 cases.	